Force induced dissociation of molecular bonds

van Donkelaar, I.M.A.

Award date:
2008

Force induced dissociation of molecular bonds

I.M.A. van Donkelaar

December 2007
MBx 2007-14

Master thesis in Applied Physics
Eindhoven University of Technology

Supervisor:
dr.ir. A.M. de Jong

Research group:
Molecular biosensors for medical diagnostics

Abstract

Antibodies are important molecules for medical diagnostics and medical treatment. There is a need for technologies to rapidly test the quality of antibodies. A measure for the quality of an antibody is given by the rate at which it dissociates from the antigen to which it is specifically bound. To be able to obtain a fast quantification of this rate, force induced dissociation of molecular bonds is studied using superparamagnetic beads.

Superparamagnetic beads with a diameter of 2.8 μm coated with receptor molecules are bound to a surface with ligand molecules. A setup has been developed in which forces up to 90pN can be exerted on the beads. These forces can be either constant or increased at loading rates up to 10pN/s. Optical detection is used to observe the decrease in the number of beads that is bound to the surface as a function of time. With this setup measurements on the force dependance of the dissociation rate of two molecular bonds, the Biotin-Streptavidin and the Biotin - Anti-Biotin bond, have been performed.

Biotin, coupled to a Bovine Serum Albumin protein, was immobilized on a polystyrene surface via adsorption. Beads with Streptavidin or Anti-Biotin covalently coupled to it were bound to the surface immobilized Biotin.

Dissociation measurements at constant forces have shown that the dissociation rate increases with the applied force, which is expected from theory. The shape of the dissociation curves indicates, that both Anti-Biotin and Streptavidin coated beads often bind to the Biotin-BSA surface with more than one specific bond. The average number of bonds however is lower in case Anti-Biotin is used.

A fast dissociating fraction of Streptavidin coated beads is observed that is not expected from literature. Possibly this fraction of beads is only partially bound. The shape of the dissociation curves of the Streptavidin coated beads corresponds to a situation in which Biotin-Streptavidin bonds between the bead and the surface are parallel and break randomly.

Dynamic Force Spectroscopy (DFS) measurements have been performed on the Biotin - Anti-Biotin bond. From these measurements possible dissociation rates at zero force of, $7.7 \cdot 10^{-3}$, $1.9 \cdot 10^{-2}$ and $1.1 \cdot 10^{-4}$ s^{-1} are derived, which are all much higher than the dissociation rate of $5.8 \cdot 10^{-6}$ s^{-1} reported in literature. The dissociation rate at constant forces, calculated from the parameters derived from DFS experiments, does not match the dissociation measured in constant force experiments. Possibly the data obtained in DFS experiments is insufficient to be interpreted correctly.

In general deriving quantitative information from the conducted measurements was difficult because of the occurrence of multiple bonds per bead, the low number of beads dissociating and irreproducibilities. These causes are mostly of biochemical origin. For better results optimization of the biochemistry is essential.

Table of contents

Chapter 1

Introduction

The research presented in this report has been conducted in period of January 2007 until December 2007 as a graduation project within the research group Molecular biosensors for medical diagnostics (MBx) at the Technical University of Eindhoven (TU/e). The group MBx is established in October 2005 in close cooperation with Philips Research and is especially focussing on magnetic biosensors. This project, which has as a goal to develop a method to measure bond strengths of antigen-antibody complexes, contributes to the more wide defined mission of the group of investigating new technologies for sensitive biological detection in small sample volumes. In this introductory chapter some further background is given on biosensors in general and magnetic biosensors in specific. Furthermore the possible application of magnetic biosensors in determining the strength of antigen-antibody bonds is discussed. The chapter is concluded with an outline of the rest of this report.

1.1 Magnetic biosensors

A biosensor is a device that is used to detect the presence or concentration of certain biological molecules, for example proteins or sugars, in body fluids. Because the presence of such a molecule can usually not be detected directly, a labeled complement (receptor), of the molecule to be detected (ligand) is often needed. This labeled receptor binds uniquely to that ligand with a high bond strength. Such a bond that is characterized by its high strength and uniqueness is called a specific bond. The formed ligand-receptor complex can be detected by its label. The final step before the actual detection is the separation of complexes and excess labeled receptor. There are various types of biosensors available on the market, using different mechanisms of labeling, separation and detection.

A magnetic biosensor concept [1] has been developed by Philips in which superparamagnetic beads are used as a label. Superparamagnetic beads can

be strongly magnetized in the presence of a magnetic field which enables their detection with a magnetic sensor, for example a GMR or a Hall sensor. Using magnetic labels enables sensitive biosensing as the magnetic background in biological samples is low. Without the presence of a magnetic field the beads do not stay magnetized, therefore they will not form unwanted aggregates.

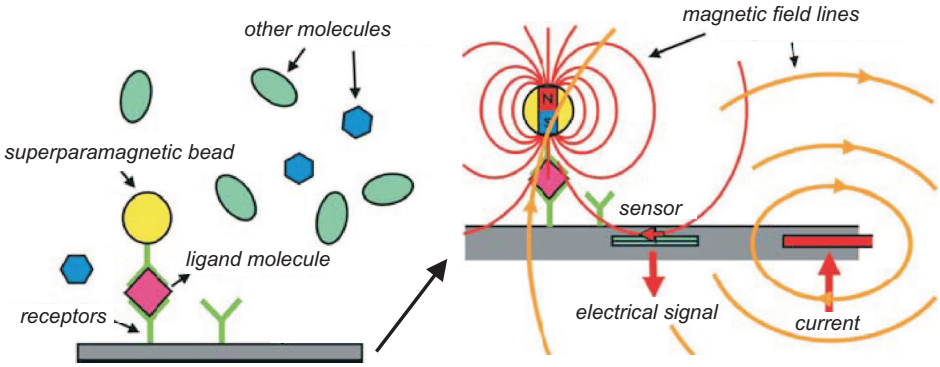

Figure 1.1: Binding and detection in the Philips magnetic biosensor. This figure is not to scale, in reality the dimensions of the superparamagnetic beads are much larger than those of the detected molecules. Figure adapted from [2].

In the Philips biosensor the superparamagnetic beads covered with receptor molecules are incubated in a solution containing the ligand. As the beads are suspended in the solution and have a large surface area the average distance between ligand in the solution and a receptor is smaller than if the receptors were on a flat surface. Therefore the incubation is faster. The beads that have bound a ligand are separated from the rest by binding them to a surface which is coated with a receptor that binds to another part of the ligand, see the left side of figure 1.1. The beads that did not bind a ligand can not bind to the surface and are washed away together with possible excess ligand. The amount of beads bound on the surface, scales with the concentration of ligand in the solution. It can be measured by a GMR sensor embedded in the surface when the beads are magnetized by sending a current through wires also embedded in the surface, see the right side of figure 1.1. The GMR sensor is only sensitive to components of the magnetic field parallel to the surface. The magnetic fields induced by the current wires are perpendicular to the surface at the position of the GMR and do not affect the measurement.

To speed up the binding of beads to the surface, the superparamagnetic

beads can be used as actuators. By exposing the beads to a magnetic field gradient a force can be applied to them to pull them towards the surface.

1.2 Magnetic biosensor with extended functionality

The use of superparamagnetic beads as actuators can be extended to other applications. Once a bead is bound to a surface via a ligand-receptor bond, this bond can be broken by applying a force on the bead directed away from the surface. The effect of a force on the lifetime of a bond is a measure for the strength of the bond. The bond strength between a ligand and a receptor is a measure for the quality of the receptor.

A specific type of ligand-receptor bond for which it could be interesting to know the bond strength is the antigen-antibody bond. Antibodies, also called immunoglobulins, are proteins produced by the immune system to recognize and bind to target molecules, also called antigens, which could be harmful to the body. The binding site of an antibody is composed of a large number of amino acid sequences and binds with a high degree of specificity to an antigen. As there are 22 amino acids the number of variations in binding sites is large. Therefore a large variety of antigens can be recognized.

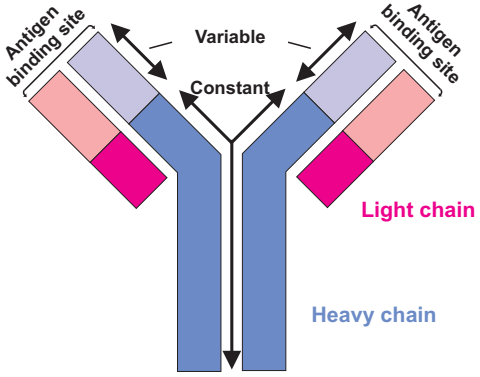

Figure 1.2: Schematic picture of an antibody.

There are five different classes of antibodies, IgA, IgD, IgE, IgG and IgM, of which IgG is the most abundant. A schematic picture of an IgG antibody is given in figure 1.2. An IgG molecule is Y-shaped and consists of two identical heavy and two identical light (amino acidic) chains that all have a part that is the constant in every IgG molecule and a part that varies. The variable part of the chains is located at the antigen binding sites. Each IgG molecule has two identical binding sites at the tips of the Y. The bottom part of the Y is called the crystallisable fragment of the antibody.

There are diseases for which bond strength of antibodies against the disease antigen in the body are a measure for the severity of the disease. To probe the development of such diseases it is not only necessary to measure the concentration of antibodies but also their bond strength. The production of bioactive immune milk is an another example of a process in which it is important to know the strength of the bond between an antigen and an antibody. Bioactive immune milk contains high concentrations of antibodies against a certain type of antigen. Consumption of this milk helps preventing symptoms related to that antigen. Immunized cows are used in the production process of these antibodies, the antibodies are secreted in their milk. The concentration and quality of the secreted antibodies varies per cow and in time. To prevent good quality an bad quality milk being mixed, a sensor is needed in which both the concentration and the quality, reflected by the bond strength, of the produced antibodies can be tested per cow during milking. In this case it is not feasible to send milk samples to a lab and receive the results a day later.

There is thus a need for a fast biosensor that can do more than only measuring concentration. The functionality of the biosensor should be extended with the possibility to measure bond strengths. Superparamagnetic beads can play a double role in such a sensor because they can be used as labels as well as actuators. Furthermore for the magnetic actuation of the beads themselves no physical contact with a transducer is needed which gives the system a certain robustness.

1.3 This research project

The research presented here, focusses on the use of superparamagnetic beads for fast quantification of bond strengths, for future implementation in a biosensor system. A measure for the strength of a ligand-receptor bond is given by the rate at which it dissociates. A setup has been developed by which the force induced dissociation of molecular bonds between a superparamagnetic bead and a surface can be studied. In this setup both constant forces and forces that are increased at a steady loading rate can be applied to the beads.

The Biotin-Streptavidin system is initially used as a model system for the antigen-antibody interaction. The Biotin-Streptavidin bond is the strongest known non-covalent bond, and the (force induced) dissociation of this bond has been studied intensively [3] [4] [5].

Biotin is a vitamin with the chemical formula $C_{10}H_{16}N_2O_3S$. It is a relatively small water soluble molecule. The chemical structure of Biotin is shown in figure 1.3(a). The molar mass of biotin is 244.31 g/mol. In the human body the biotin is a catalyst for some important metabolic reactions.

The Streptavidin protein molecule is a tetramer consisting of four identi-

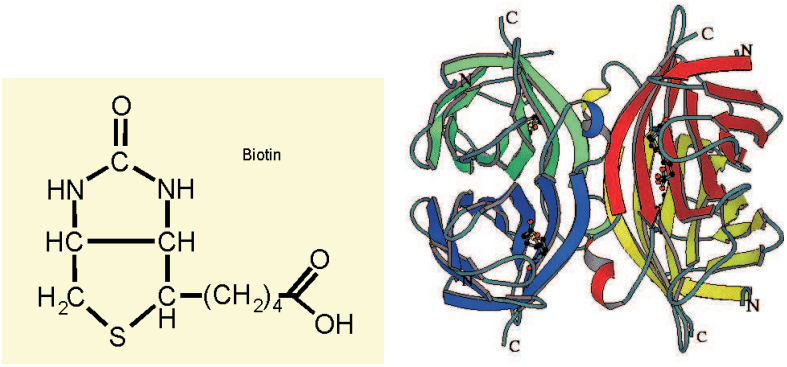

(a) (b)

Figure 1.3: (a) Chemical structure of Biotin. (b) Streptavidin protein structure [6].

cal 13 kg/mol subunits that each have a binding site for Biotin. The protein structure of Streptavidin is shown in figure 1.3(b). In a crystalized form the dimensions of a Streptavidin molecule are 10 x 10 x 12.6 nm [7]. The disadvantage of using the Biotin-Streptavidin system is that it is hard to obtain a single Biotin-Streptavidin bond between a bead and a surface since one Streptavidin molecule already has four binding sites.

The probability of binding by multiple bonds is less for antibodies that have only two binding sites. Therefore also measurements on the Anti-Biotin - Biotin system have been performed. Anti-Biotin is an antibody of the IgG class. The size and molecular weight of this type of antibody is comparable to that of a Streptavidin molecule. In this project Anti-Biotin molecules raised in goats have been used.

1.4 Outline

In the next chapter of this report, the nature of ligand-receptor bonds is explicated. It starts with a description of the most important non specific interactions. Subsequently the kinetics of ligand-receptor bond formation in solutions is discussed. Effects that occur when a force is applied to a single ligand-receptor bond are described in the final section of this chapter. Two special cases are considered: the case that a constant force is applied and the case that a force is applied that is increased at a steady loading rate.

In chapter three the experimental setup that has been developed to enable the study of force induced dissociation of ligand-receptor bonds is described. With this setup measurements have been performed on two different systems: the Biotin-Streptavidin system and the Biotin - Anti-Biotin

system. How the mentioned molecules are immobilized on a surface or on superparamagnetic beads is also described in this chapter as well as the properties of the superparamagnetic beads.

Chapter four contains the results of measurements on the Biotin-Streptavidin system. All measurements on this system have been performed at a constant force. Chapter five contains the results on the Biotin - Anti-Biotin system. On this system both measurements at forces constant in time and forces that are increased at a steady loading rate in time have been performed.

The final chapter of this report summarizes the conclusions. Furthermore the possibilities for implementation of force induced dissociation measurements in a biosensor are discussed.

Chapter 2

Ligand-receptor bonds

In this chapter the theory behind ligand-receptor bonds is described. Ligand-receptor bonds are bonds between two molecules that are highly specific in their interaction. Specificity is generally characterized by two aspects, a high binding strength and a unique binding site. However the distinction between specific and non-specific binding is rather arbitrary. [4] Specific bonds arise from a unique combination of non-specific interactions occurring consecutively and/or simultaneously. The first section of this chapter focusses on the properties of non-specific interactions that enable ligand-receptor binding. Section 2.2 covers spontaneous association and dissociation of antibodies and antigens in solution, while in 2.3 the force induced dissociation of molecular bonds is treated.

2.1 Non-specific interactions

Because specific bonds arise from non-specific interactions, it is important to understand these interactions. Furthermore, as in the research presented in this report the specifically binding molecules are attached to macroscopic surfaces, also the non-specific forces between these surfaces are of importance. Therefore the nature of the major non-specific interactions will be explained in this section.

2.1.1 Van der Waals interaction

The Van der Waals interaction is a generic term for three different types of interactions: Keesom, London and Debeye interactions. The common property of these interactions is that they all arise for an uneven charge distribution over molecules. Molecules that have an uneven charge distribution are called polar molecules. When two polar molecules approach, Keesom forces will orient the molecules in their energetically most favorable direction. When a polar molecule approaches a non-polar molecule it can induce

an uneven charge distribution in that molecule. The forces associated with this interaction are called Debeye forces. The last type of Van der Waals forces is the London dispersion force. This force is present between two non-polar molecules due to fluctuations in their charge distribution which become correlated when the molecules approach each other.[8]

On a microscopic scale the Van der Waals interaction energy between two molecules is given by:

$$e(d) = \frac{-C}{d^6}, \tag{2.1}$$

in which C is a constant depending on material properties and d is the separation distance between the molecules. In this equation retardation and multipole interactions, that would give rise to additional terms depending on higher powers of d, are neglected [8]. From this microscopic interaction energy the interaction energy between two macroscopic bodies can be calculated using pairwise additivity by integration over all molecules in the macroscopic bodies. For the specific geometry of two half spaces/flat plates the resulting expression for the energy per unit area becomes:

$$E^{vdw}(d) = \frac{-\pi^2 C \rho_1 \rho_2}{12 d^2} = \frac{A_{12}}{12\pi d^2}, \tag{2.2}$$

where ρ_1 and ρ_2 are the number densities of atoms in the two half spaces and A_{12} is the Hamaker constant for two bodies 1 and 2 interacting across vacuum. In most experimental situations two bodies do not interact across a vacuum but across some other medium. In the research project described here a bead interacts with a surface across a watery solution. This medium modifies the Van der Waals interactions. The expression for the Hamaker constant, A_{132}, for two bodies 1 and 2 interacting across another medium 3, derived using additivity is given by [8]:

$$A_{132} = A_{12} + A_{33} - A_{13} - A_{23} = (\sqrt{A_{11}} - \sqrt{A_{33}})(\sqrt{A_{22}} - \sqrt{A_{33}}), \tag{2.3}$$

in which A_{ii} represent the interaction energies across vacuum. Because of reflection of fluctuating electric fields generated by an interacting pair of molecules by molecules of the medium, the interaction gets enhanced. Therefore when pairwise additivity is used to derive the Hamaker constants for two bodies interacting across an other medium this gives an underestimation of the interaction energies.

Another approach in the determination of A_{132} is using Lifshitz's theory. Lifshitz does not take the microscopic properties of the material as a starting point, instead the macroscopic bodies are considered and the Maxwell equations are applied to them [9]. The result of this approach is a composite Hamaker constant expressed as a function of the dielectric permittivities of the materials involved.

Independent of the way in which the composite Hamaker constant is derived, the energy of interaction per unit area for two half spaces 1 and

2 interacting across another medium 3 is similar to equation 2.2 only this time A_{12} is replaced by A_{132}.

2.1.2 Electrostatic interaction

Electrostatic interactions act between charged surfaces. When a surface is in contact with an electrolyte it can attain surface charge by adsorption of ions from the liquid or ionization of surface groups. The surface charge generates an electrostatic field which influences the ions in the bulk of the liquid. To compensate for the surface charge, a number of counter ions will also adsorb to the surface. The counter ions are of a finite size so can not approach the surface closer than a certain distance, r, approximately corresponding to their molecular radius. The layer that is not accessible to counter charges is called the Stern layer. The layer of counter ions outside the Stern layer is called the diffuse layer. In this layer the charge density will follow a Boltzmann distribution [10]. A schematic picture of the described layers is given in figure 2.1.

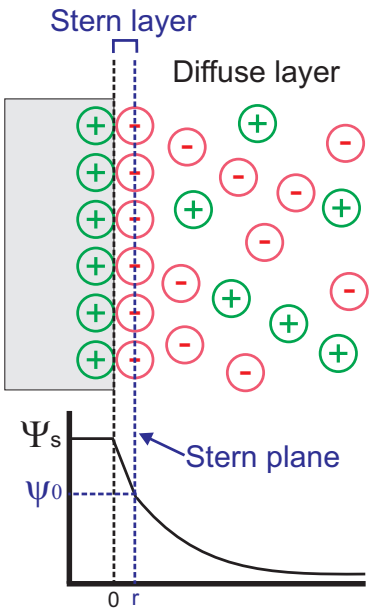

Figure 2.1: Schematic picture of the potential and charge distribution close to a charged surface in an electrolyte. Here Ψ_s is the surface potential and ψ_0 is the potential at the Stern plane.

The electrostatic interaction can be quantified by solving the Poisson-Boltzmann equation. In the case of an electrolyte in which the positive and negative ion are present in the same concentration and have the same charge number, the Poisson-Boltzmann equation for a flat surface can be expressed as [11]:

$$\frac{d^2\Psi(x)}{dx^2} = \frac{-2zen}{\varepsilon}\sinh(\frac{ze\Psi(x)}{k_BT}), \tag{2.4}$$

where $\Psi(x)$ represents the electrostatic potential as a function of the distance, x, from the Stern plane (see figure 2.1), n is the bulk concentration of ions, z is its charge number, e is the elementary charge, ε is the permittivity of the electrolyte, k_B is the Boltzmann constant and T is the temperature.

This equation can be solved analytically and under the assumption of small electrostatic potentials, this yields the following expression for the

electrostatic potential [12]:

$$\Psi(x) = \frac{4k_BT}{ze} \tanh \frac{ze\psi_0}{4k_BT} \exp -\kappa x, \tag{2.5}$$

in which ψ_0 is the surface potential at the Stern plane. Here κ is the inverse of the Debeye length which gives the decay length of the interaction, and is given by:

$$\kappa = (\frac{2z^2e^2n}{\varepsilon k_BT})^{1/2}. \tag{2.6}$$

The electrostatic energy of interaction between two planar surfaces with such an electrostatic potential would be [4] [12]:

$$E^{es}(d) = \frac{\kappa}{2\pi} Z \exp -\kappa d. \tag{2.7}$$

Z is given by:

$$Z = 64\pi(\frac{k_BT}{ze})^2 \varepsilon \tanh \frac{ze\psi_0^1}{4k_BT} \tanh \frac{ze\psi_0^2}{4k_BT}, \tag{2.8}$$

in which ψ_0^1 and ψ_0^2 are the potentials at the Stern plane of the two interacting surfaces.

2.1.3 Hydrophobic and hydration interaction

Hydrophobic and hydration interactions are important if molecules or particles are dissolved in water. They originate from the interaction between water molecules via hydrogen bonds that are essentially very strong dipole-dipole interactions. The interaction energy depends on the hydrophobicity (or hydrophillicity) of the molecule or particle surface. The hydrophobicity of a molecular group is a property that relates to how well this group can interact with water via dipole-dipole interactions. Polar groups have a stronger interaction with water and are more hydrophillic than non-polar groups which are more hydrophobic. When the hydrophobicity of a macroscopic surface is concerned this is often quantified in terms of the contact angle that the surface of a water droplet makes with it, see figure 2.2. Roughly if the contact angle is larger than 90^o the surface is said to be hydrophobic, if it is between 75^o and 90^o it is partially hydrophobic and if it is smaller it is hydrophilic [4].

Attractive forces between two hydrophobic surfaces develop because the energy of interaction between two water molecules is higher than between a water molecule and the surface. Although the exact mechanism of this interaction is not known, it has been suggested that a depletion layer of water forms around hydrophobic surfaces, see figure 2.3a. When the depletion layers of two surfaces overlap this would give and under-pressure in the depleted region leading to attraction between the two surfaces [4] [13].

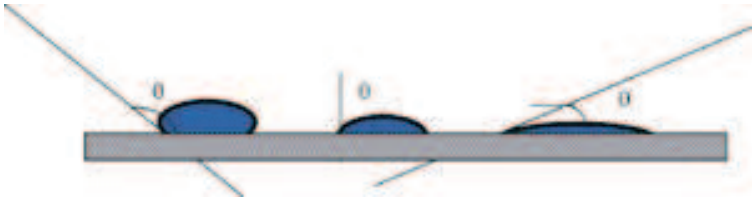

Figure 2.2: The contact angle, θ, with a surface is a measure for its hydrophobicity. From left to right contact angles are depicted for a hydrophobic, a partially hydrophobic and a hydrophillic surface.

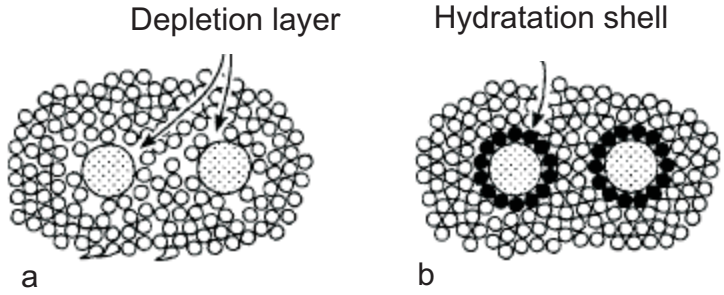

Figure 2.3: Particles (big spheres) in water (small spheres). (a) A depletion layer is formed around hydrophobic particles. (b) A hydration shell is formed around hydrophilic particles. Figure adapted from [4].

On the other hand interactions between hydrophilic surfaces in water, are mainly caused by the molecules of water that are very strongly hydrogen-bonded to the surface (the hydration shell), see figure 2.3b. A strong steric repulsion will occur in this case when the surfaces approach each other to a distance of two times the size of the water molecule. Furthermore, depending on the configuration of the water molecules, an additional monotonic repulsion or attraction will contribute to the total interaction. This contribution has an electrostatic nature as it is caused by the interaction between the water dipoles in the hydration shell [4]. In figure 2.4 the interaction between these water dipoles is depicted.

A theory in which both repulsive and attractive hydration and hydrophobic interactions are unified has been postulated by C.J. van Oss [9]. He derives the following expression for the interaction energy per unit area for two surfaces:

$$E^{hyd}(d) = E(d_0) \exp \frac{d_0 - d}{\lambda_0}. \tag{2.9}$$

Here d_0 is the minimum separation distance of the surfaces and λ_0 is the decay length of the interaction which is about 1 nm. The interaction energy

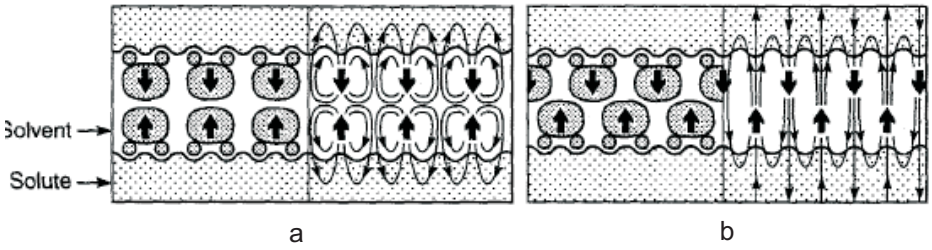

Figure 2.4: Two possible configurations of water (solvent) molecules in the hydration shells. (a) The water molecules are exactly opposing each other, this leads to a monotonic repulsion. (b) The water molecules are staggered and their dipoles complement each other, this leads to a monotonic attraction. Figure adapted from [4].

at the minimum separation distance, $E(d_0)$, is a parameter that can be derived from contact angle measurements [9].

2.1.4 Adhesion force

When two elastic bodies, like protein coated beads and surfaces, interact with each other they will deform. The contact area of those bodies can be calculated using the theory develloped by K. L. Johnson K. Kendall and A. D. Roberts (JKR theory) [14] in which the assumed deformation is flattening or stretching. When an attractive interaction is present between such bodies in contact they will flatten until there is a certain equilibrium contact area. If now a force is exerted on one of the bodies to pull it away from the other body, the deformation will change and the bodies will be stretched. At a certain force, the adhesion force f_a, the strength of adhesion (in case of attractive interaction) will be insufficient to support the deformation. At this force the surfaces will jump apart. According to JKR theory the relation between the radius of the contact area, a, and the applied force, f, between a sphere with radius R and a surface is given by [4]:

$$a^3 = \frac{R}{K}(f + 6\pi R\gamma + \sqrt{12\pi R\gamma f + (6\pi R\gamma)^2}), \tag{2.10}$$

where K is a measure for the elasticity of the surfaces and γ is the interfacial energy which is related to the total energy of interaction per unit area via:

$$\gamma = \frac{1}{2}(E^{vdw}(d) + E^{es}(d) + E^{hyd}(d) + ...). \tag{2.11}$$

The adhesion force that follows from equation 2.10 is given by:

$$f_a = -3\pi R\gamma. \tag{2.12}$$

This force scales with the radius of the sphere. Note that the assumed deformation of the bodies is based on bodies with a uniform elasticity. A protein coated bead has a relatively hard core and an elastic protein surface, which is mainly the part in which deformation takes place. The thickness of the elastic surface does not vary with the radius of the bead. Therefore the increase in contact area with the radius is expected to be smaller than assumed in equation 2.10, as a consequence also the dependence on the radius in equation 2.12 is expected to be overestimated.

The model described here is only relevant when macroscopic systems are concerned, which are composed of many molecules and show only slow dynamic changes on the timescale of a force measurement. If however individual molecular pairs are investigated the dynamics are often very fast and governed by the thermal energy of the molecules. This gives rise to time dependent and statistical behavior which will be further discussed in section 2.3.

2.1.5 Interactions comprised in the Biotin - Streptavidin bond

The binding mechanism for Biotin and Streptavidin has been investigated using crystallographic methods [7][15]. Three different mechanisms are identified that contribute to the strong ligand receptor bond. In the first stage of binding, hydrophobic and Van der Waals interactions between the biotin and four tryptophan amino acidic side chains in the Biotin binding site, direct the Biotin towards the binding site and orient the Biotin molecule. Once in the binding site the biotin molecule is fixated in a network of hydrogen bonds. Finally a loop of amino acids at the surface of the Streptavidin molecule folds over the ligand resulting in the Biotin being captured inside the Streptavidin. In figure 2.5 the process of Biotin binding is drawn schematically.

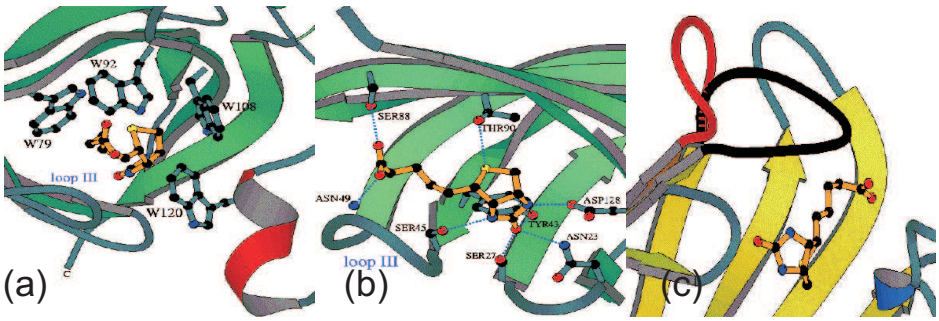

Figure 2.5: Biotin (orange molecule) binding to Streptavidin [15]. (a) Biotin is attracted towards the binding site. (b) Hydrogen bonds are formed. (c) A loop of amino acids folds over the Biotin in the binding site.

What makes this interaction specific is the complementarity of the Biotin and the binding site on many levels: the shape of the binding site is matched to the Biotin molecule, the local distribution of charges is such that a negative charge on the biotin molecule is close to a positive charge in the binding site furthermore the positions where hydrogen bonds can be formed in the binding site are adjusted to the molecular structure of Biotin.

2.2 Kinetics of binding in solutions

The formation of a complex from a ligand and a receptor in general or an antibody and an antigen in specific is often considered to be a reversible reaction that occurs in a single reaction step and with a single transition state. The transition state is the state with the highest energy that has to be overcome during the reaction.

$$antigen + antibody \rightleftharpoons complex$$

Starting from the rate equation for such a reaction, the rate of complex formation in a solution and equilibrium conditions are derived in section 2.2.1. How the derived expressions can be used to fit experimental results in order to determine the rate and equilibrium constants of the reaction is shown in 2.2.2.

2.2.1 Basic equations

In a solution containing a mixture of an antigen and its antibody the following differential equation gives an expression for the time dependence of the concentration of antibody-antigen complexes, x, present in the solution:

$$\frac{dx}{dt} = i \cdot a \cdot k_{on} - x \cdot k_{off}, \tag{2.13}$$

in which i is the concentration of free antibodies i.e. antibodies that don't have an antigen bound to it, a is the concentration of free antigen, k_{on} $[M^{-1}s^{-1}]$ and k_{off} $[s^{-1}]$ represent the association rate and dissociation rate constant respectively. The concentrations of free proteins in the solution relate to the concentration of complexes via $i = i_0 - x$ and $a = a_0 - x$, in which i_0 and a_0 are the total concentrations of antibody and antigen respectively.

In equilibrium $\frac{dx}{dt} = 0$ and thus $i \cdot a \cdot k_{on} = x \cdot k_{off}$ or in a rewritten form:

$$\frac{x}{a \cdot i} = k_{on}/k_{off} = K, \tag{2.14}$$

where K $[M^{-1}]$ is the equilibrium constant which is a measure for the affinity of the antibody for the antigen. A high affinity indicates a strong bond between the antigen and the antibody. Affinity is related to single bonds.

When an antibody can bind to an antigen by more than one bond, the term avidity is used to quantify the total effectiveness/strength of binding instead.

In general both k_{on} and k_{off} should be known to say something about strength of a bond. However in the case of an antigen-antibody bond the differences in k_{on} between different antigen-antibody pairs are rather limited. k_{on} is usually in the order of $1{\cdot}10^7 M^{-1}s^{-1}$ whereas k_{off} varies widely between $1{\cdot}10^{-4}$ and $1{\cdot}10^4$ s^{-1} for antigen-antibody pairs with various affinities [16]. As k_{on} does not vary so much, k_{off} largely determines the affinity. The antigen-antibody bond strength can thus be quantified by its dissociation rate constant.

Under the circumstance that association can be neglected, equation 2.13 simplifies to:

$$\frac{dx}{dt} = -x \cdot k_{off}. \tag{2.15}$$

Integration of this equation gives:

$$x = x_0 \exp(-k_{off}t), \tag{2.16}$$

in which x_0 is the concentration of complexes at $t = 0$.

If the total concentration of antigen in the solution is much larger than the concentration of antibody, the concentration of antigen can be assumed constant during the process of reaching equilibrium. The fraction that binds to or is released from (depending on the starting conditions) the antibody in that case is negligible compared to the total antigen concentration. Solving equation 2.13 assuming a constant antigen concentration $a = a_0$ and taking a starting condition of $x = 0$ at $t = 0$ yields:

$$x = \frac{a_0 \cdot i_0}{a_0 + 1/K}(1 - \exp(-(a_0 \cdot k_{on} + k_{off})t)). \tag{2.17}$$

A starting condition of $x = i_0$ at $t = 0$ yields:

$$x = \frac{i_0(a_0 \cdot K + \exp(-(a_0 \cdot k_{on} + k_{off})t))}{a_0 \cdot K + 1}. \tag{2.18}$$

Equations 2.16, 2.17 and 2.18 are often used in the determination of k_{on} and k_{off}.

2.2.2 Measuring rate and equilibrium constants

k_{on} can be derived from measurements of a response Rx proportional to the concentration of antibody-antigen complexes x as a function of time for different antigen concentrations a_0 keeping the number of antibodies constant and small. By fitting Rx versus time with the equivalent of equation 2.17 for Rx instead of x, the term $a_0 \cdot k_{on} + k_{off}$ in the exponent can be found.

Plotting this term versus a_0 results in a straight line with a slope of k_{on}. Theoretically k_{off} could be determined from the intercept of this line with the vertical axis, however this method is only accurate for high values of k_{off}. Otherwise, if k_{off} is orders of magnitudes smaller than k_{on} (which is often the case), a small error in k_{on} leads to large error in k_{off}.

A faster method of measuring k_{on} is using initial rate analysis. Here the slope of the first, linear, part of the Rx versus time curve is plotted against a_0. Again this leads to a straight line, this time with a slope of $k_{on} \cdot Ri_0$ and an intercept of 0. Here Ri_0 is the measured response in case the antibodies in the system are saturated with antigen and thus $x = i_0$. For a derivation of this, see [17]. This method only works if k_{off} is sufficiently small, because a larger k_{off} leads to a smaller linear part in the Rx versus time curve. How small this part can become before it is to small to be probed depends on the specific technique used to probe the interaction.

The dissociation rate constant can be determined by measuring Rx as a function of time under the condition that association is negligible. This condition can be met by bringing the concentration of free antigen to far below 1/K so the probability for association is very low, or by labeling only the antigen that is initially bound to an antibody and than adding a high concentration of unlabeled antigen. If this concentration is high enough it will block all unoccupied antigen sites preventing binding and rebinding of the labeled antigen. Fitting the Rx versus time curve with the equivalent of equation 2.16 for Rx instead of x, will give a value for k_{off}. When k_{off} is small this type of measurement is time consuming. For example the half-life of the Biotin - Streptavidin complex, having a k_{off} of $\sim 10^{-5}\ s^{-1}$, is about 20 hours.

The equilibrium constant can be calculated from the dissociation and association rate constant once these have been measured. It is also possible to measure K directly. In contrast to the dissociation and association rate constants the equilibrium constant is not measured in the kinetic (time dependant) regime of the antigen antibody interaction. The measurements needed to determine K are done after equilibrium has been established. The time it takes to reach equilibrium depends on the concentrations of antigen and antibody and on the rate constants. Especially at low concentrations the time before reaching equilibrium can be very long. For example, the time it takes for the Biotin-Streptavidin system to approach to 99% of its equilibrium complex concentration is about 67 hours, at an antigen concentration of $\frac{1}{K}$ and an antibody concentration $< \frac{0.01}{K}$.

Determining K is often done by making so called Scatchard plots, based on the Scatchard equation [18] which is the equilibrium equation 2.14 in a rewritten form:

$$\frac{x}{a} = K(i_0 - x). \tag{2.19}$$

In a Scatchard plot $\frac{x}{a}$ is plotted versus x resulting in a straight line with

a slope of K. To do so the bound and the free concentration of antigen must be measured for different starting concentrations of antigen. This involves separation of the bound and the free fraction of antigen. If the total concentrations of antigen and antibody during the experiment are known only one of the fractions needs to be measured. The other fraction can be calculated from that.

There is a broad range of techniques that is used to measure the concentration of a certain antigen, antibody or complex. Most of these techniques use labeled antigens or labeled antibodies, some involve the attachment of either the antibody or the antigen to a solid support. Examples of techniques that are commonly use are: Enzyme Linked ImmunoSorbent Assay (ELISA), Surface plasmon Resonance (SPR), Fluorescence Polarization (FP) and Radio Immuno Assay (RIA). For more information about these techniques see reference [19].

2.3 Force induced dissociation

In the previous section the strength of a bond between an antigen and antibody was defined in terms of how fast it associates and dissociates naturally. There is however a different way of looking at the strength of a bond, that is to which extend it can resist a force that is applied to it. Here it is important to keep in mind the nature of the bond. As is described in the previous section, an antigen-antibody bond will dissociate eventually even if no force is applied. Investigating at which force the bond will break does not make sense in that respect, as a bond will break at any force. However a force applied to this type of bond will influence the lifetime of the bond.

When an isolated antibody antigen pair is considered it can either be in the bound state or be detached. For a large ensemble of such isolated pairs, the probability for a pair to be in the bound state as a function of time is given by the following differential equation [20]:

$$\frac{dS_1}{dt} = S_0(t) \cdot k_a(t) - S_1(t) \cdot k_d(t). \tag{2.20}$$

In this equation S_1 is the probability to be in the bound state, $S_0 \equiv (1 - S_1)$ is the probability to be in the unbound state, k_d $[s^{-1}]$ and k_a $[s^{-1}]$ represent the rates of the transitions between the two states. Different symbols for the rate constants are chosen than in equation 2.13. The association rate constant, k_a, is essentially different from k_{on}. It also has different units as in this case there is no ambient concentration of antigen playing a role in the rate of association. The dissociation constant, k_d, has the same units as k_{off} and describes the same process. However for clarity k_d will be used in the remainder of this report in case force dependant dissociation is considered. The value of k_d when no force is applied corresponds to k_{off}.

For an initially bound pair, the probability that the bond will be broken after a certain time follows from equation 2.20 and depends on k_d and k_a. If now a force is applied to the bond, and the antibody and antigen are pulled apart fast enough to prevent reassociation after the bond is broken, the probability for bond rupture after a certain time does then only depend on k_d. In its turn k_d is a function of the applied force, if a larger force is applied it is more probable that the bond will break faster.

To determine the dissociation rate many bond rupture events have to be monitored. Because of the statistical nature of bond breaking, conclusions can not be drawn from one breaking bond.

2.3.1 Single molecular bond

A single molecular bond can be looked upon as being in a confined state in which it is in an energy minimum. Escape from this confined state can happen along a preferential path which is represented by the reaction coordinate, x. This preferential path is not related to a one dimensional translation along a certain axis, it represents a succession of different orientations and separations of the involved molecules in 3D space. Along the reaction coordinate an energy barrier has to be overcome. Experimentally the dissociation rate constant for such an escape process was found to follow Arrhenius behavior [21]:

$$k_{off} = \nu \exp \frac{-E_b}{k_B T}, \tag{2.21}$$

in which E_b represents an activation energy corresponding to the height of the energy barrier mentioned earlier and ν is an attempt frequency factor in which essentially all dynamics of the molecules are captured. In liquids this frequency is of the order of magnitude of $10^{10} s^{-1}$ [20]. Expressions for the dissociation rate constant of the same functional shape can also be derived theoretically using transition state theory (TST) or Kramers theory [22]. From these theories a more physical expression for the attempt frequency follows. In this stage of the research a further explication of this frequency is however not necessary.

A simple expression for the force dependance of the dissociation rate constant k_d has been introduced for the interaction between two cells by Bell [23]. A similar expression can be applied to a molecular bond. This expression is based on the assumption that when a force is applied to the bond the energy barrier that has to be overcome gets lowered by $x_\beta f$, where x_β is the projection of the reaction coordinate at the position of the barrier along the direction of the force and f is the applied force. A schematic representation of this is given in figure 2.6. Substituting this force dependant barrier height in equation 2.21 gives:

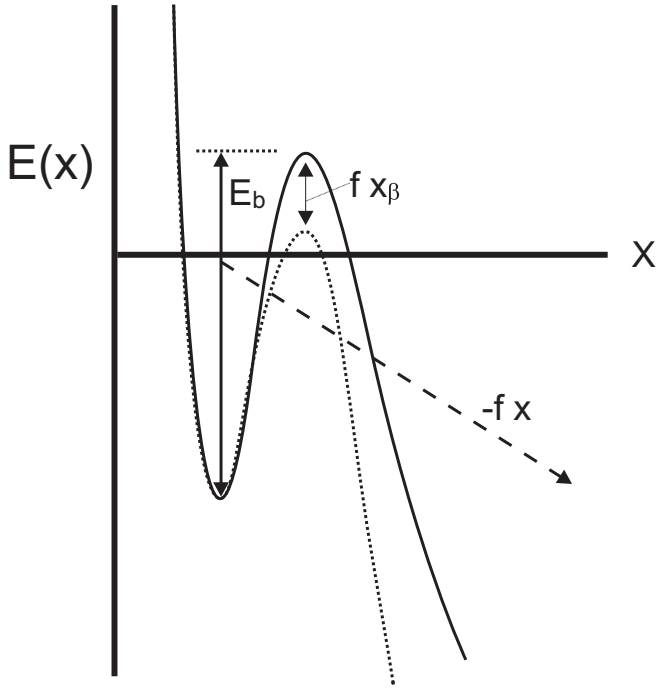

Figure 2.6: Energy landscape of a bond with a single barrier. If a force is applied the energy landscape gets tilted and the barrier is lowered.

$$k_d(f) = k_{off} \exp \frac{x_\beta f}{k_B T} = k_{off} \exp \tilde{f}, \tag{2.22}$$

in which $\tilde{f} = \frac{x_\beta f}{k_B T}$ is the dimensionless force. The dissociation rate constant thus increases exponentially with the applied force. This force dependance is only valid if the barrier is sharp and its top stays at the same position when force is being applied. This is not necessarily valid for a ligand-receptor bond, that is why effort is put into finding new (microscopic) models that describe bond rupture [24] [25]. Nevertheless, the Bell model in many cases has turned out to describe bond rupture events accurately [20], including the Biotin-Streptavidin case, and will be applied in the remainder of this report.

2.3.2 Dynamic force spectroscopy

In Dynamic force spectroscopy (DSF) the force at which a biological bond most probably breaks, when a force that is increased at a constant loading rate is applied to the bond, is determined. Testing the bond force over a broad range of loading rates is necessary as it has turned out that when

different loading rates are applied to the same bond, different values for the most probable rupture force are obtained [26]. Why this is the case can be derived using equations 2.20 and 2.22.

Under the assumption that the antigen and antibody are pulled apart fast enough so association is negligible, equation 2.20 simplifies to

$$\frac{dS_1}{dt} = -S_1(t) \cdot k_d(t). \tag{2.23}$$

A force that is increased at a steady loading rate, r_f, is applied:

$$\tilde{f}(t) = \tilde{r_f} \cdot \frac{t}{t_{off}}, \tag{2.24}$$

here $\tilde{r_f} = \frac{x_\beta r_f}{k_B T k_{off}}$ represents the dimensionless loading rate and $t_{off} = k_{off}^{-1}$. The assumption that association can be neglected is valid if $r_f > \frac{k_B T}{x_\beta t_{off}}$ [20].

When a time dependent force is applied, as described in equation 2.24, equation 2.23 can be reformulated in terms of force instead of time:

$$\frac{dS_1}{d\tilde{f}} = -\frac{t_{off}}{\tilde{r_f}} S_1(\tilde{f}) \cdot k_d(\tilde{f}). \tag{2.25}$$

The probability that a bond will break at a force $\tilde{f}$, $p(\tilde{f})$ is given by

$$p(\tilde{f}) = -\frac{dS_1}{d\tilde{f}}, \tag{2.26}$$

i.e. the decrease in the probability to be bound. The force corresponding to the maximum in this probability function, the most probable dimensionless rupture force $\tilde{f}^*$, can be derived using the condition $\frac{\partial p(\tilde{f})}{\partial \tilde{f}} = 0$. Filling in equation 2.22 for the dissociation rate constant and taking a force independent loading rate, $\tilde{r_f}$, gives the following relation between the most probable dimensionless rupture force and loading rate:

$$\tilde{f}^* = \ln(\tilde{r_f}). \tag{2.27}$$

In a typical DFS experiment the distribution of rupture forces is measured for a broad range of loading rates. If now the most probable rupture force, f^*, is plotted versus the natural logarithm of the loading rate this will give a linear curve. As $\tilde{f}^* = \frac{x_\beta f^*}{k_B T}$, the projected position of the location of the energy barrier, x_β, can be derived from the slope. From the cut-of with the x-axis where the most probable rupture force is zero, the apparent dissociation rate at zero force can be obtained. The term apparent is used here because it is probable that, by the application of a force, a certain reaction pathway is selected that otherwise would not have been accessible or favorable.

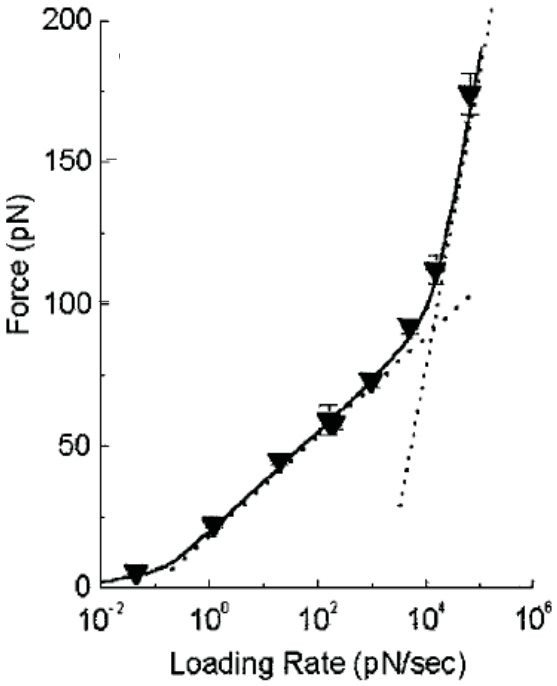

Figure 2.7: DFS spectrum of the Biotin-Streptavidin bond measured with a biomembrane force probe [3].

Merkel e.a. [3] measured the DFS spectrum of the Biotin-Streptavidin bond. The result is given in figure 2.7. They found two regions with a different slope, suggesting two energy barriers are present at projected distances of 0.12 nm and 0.50 nm along the direction of the force. These measurements have been performed using the biomemrane probe, however this type of measurements can also be done using an optical tweezer or AFM.

In AFM measurments the AFM tip is coated with one type of molecule and a surface is coated with it's complement. After a bond has been formed between the tip and the surface the tip is retracted at a constant speed which corresponds to a constant loading rate. The force on the bond is measured by the deflection of the cantilever. With this technique forces from several up to hundreds of pN can be measured at loading rates in the range of 10^{-2} pN/s - 10^{6} nN/s [4][27].

In the biomembrane probe technique for instance a red blood cell is fixed to a micropipette and a small particle is covalently attached to it. This small particle can be coated with the molecule which is to be studied. After this molecule is bound to it's complement on a surface, the pipette is retracted similarly to the AFM tip. The deformation of the red blood cell upon this retraction is a measure for the applied force. With this technique forces from 0.01 up to 1000 pN can be measured [28] at loading rates in the range of 10^{-1} - 10^{6} pN/s [4].

In optical tweezers usually molecules are fixed between a surface and a polystyrene bead. The polystyrene beads can be trapped in the focus of a laser beam and a force can be applied by shifting the position of the focus. The force is measured by characterizing the movement of the bead. With this technique forces from smaller than one pN up to hundreds of pN can be measured at loading rates in the range of 10^{-1} - 10^{3} pN/s [29].

For a more detailed description of the working principles and limitations of these techniques see reference [4]. The described techniques are all single molecule techniques making use of sensitive lab equipment. A single measurement of $\tilde{f}^*$ involves a detailed analysis of many retraction curves. It is not feasible to apply them in a biosensor.

2.3.3 Constant force application

By applying a constant force to a molecular bond, the same information as from a DFS experiment can be derived. As in this case the force is not time dependent, the solution of equation 2.23 is straightforward and yields:

$$S_1 = \exp -k_d(f)t. \tag{2.28}$$

The probability function S_1 can be probed by studying the dissociation of an ensemble of bonds. When the dissociation of a large number of beads bound to a surface by a specific bond is studied, the fraction of beads that is bound to the surface as a function of time, is equal to S_1. This fraction

of bound beads is measured in constant force measurements. $k_d(f)$ can be determined by fitting the measured dissociation curves with exponential decay.

If $k_d(f)$ is described by equation 2.22, the plot of the natural logarithm of $k_d(f)$ versus the applied force will give a linear curve. Here again x_β can be derived from the slope of the curve and the apparent dissociation constant at zero force directly follows from the intercept with the y-axis of the curve extrapolated to zero force.

For the Biotin-Streptavidin bond this type of measurements has been performed by Danilowicz e.a. [30]. In their research, as in presented research, also Streptavidin coated superparamagnetic beads are bound to a surface coated with Biotin. A force is applied to the bead by means of a permanent magnet. Instead of two barriers they find only one barrier at x_β = 0.38 nm. That a second barrier does not follow from these measurements can be because the measured force range (35 - 70 pN) is too small.

Another way of applying a constant force to a biological bond is by directing a flow along beads covered with biomolecules that are bound to an activated surface [31][32]. An advantage of pulling the beads off magnetically over pulling them of with a flow lays in the robustness of the system. This is especially important for an application in a biosensor. On the other hand the advantage of the flow method is that much smaller forces are needed to break molecular bonds because of the lever arm effect that occurs when a force is applied on the bead parallel to the surface.

The evanescent wave detection technique applied in reference [32] has as an advantage that the vertical movement of the bead can be monitored and that the force on a bead can be derived directly from this movement. This method can give more insight in the specific way a particular bead is bound to the surface. However when it is to be used to probe a probability density function for bond survival it would have to be repeated very often as only one bead is monitored at a time.

2.3.4 Multiple bonds

It is not evident that single bonds, and not multiple bonds, are measured using any of the techniques mentioned in the last 2 paragraphs. All involve two approaching bodies with dimensions much larger than the actual binding molecules. Zhu e.a. [33] discuss a number of criteria for experiments or experimental results that are commonly used in order to give confidence that a single bond is measured.

A strategy that is often used to achieve single bond events is making their occurrence infrequent by dilution of binding sites. Infrequent occurrence is however only a valid criterium for observing single bond events if the dilute binding sites are distributed uniformly over the surface, which is not necessarily the case. If there are clusters of binding sites, one attachment could

still correspond to multiple bonds. This could lead to measurement results similar to expected results for single bonds, however the interpretation of the data should be different. The derived parameters in this case correspond to the cluster instead of to a single bond. Another issue that can complicate data interpretation is surface roughness. If the dimensions of surface roughnesses are large compared to those of the molecules this may lead to differences in the accessibility of binding sites. When a molecule is difficult accessible it might be unable to form a single bond with full strength but still bind to form a partial bond.

Another criterium for the observation of single bond events is that the lifetimes of the bonds should follow single bond kinetics. The assumed kinetic mechanism in presented research is first order irreversible dissociation with an exponential distribution. It could however be possible that dissociation curves for processes other than first order irreversible dissociation, do not differ sufficiently from those expected for single bonds to be recognized in experimental results.

The given criteria are able to discriminate between single and multiple bonds if those can be diluted and when bonds with a simple kinetic mechanism, like irreversible dissociation in one step, are considered. However one still must be careful in the interpretation of data as effects of complex binding schemes, clustering and heterogeneous surfaces can be very subtle.

When irreversible dissociation in one step is the reaction mechanism for a single bond, analytical expressions can be derived for the dissociation rate constant for a multiple of these bonds [20]. In this case, if multiple bond adhesions are probed, this would lead to results of DFS and constant force experiments, that are significantly different from results for single bond behavior. Different dissociation rate constants can be defined for beads bound with a different number of bonds. How the dissociation rate constant and its force dependence for i bonds relates to that for one bond, depends on how the bonds are broken. It could be that all bonds break cooperatively, or they could break in a random way. Further it matters if the bonds are in series or parallel.

In case of i bonds in series that break cooperatively the dissociation rate is given by [20]

$$k_d^i == \frac{\exp -i\tilde{f}}{t_{off}^i}, \tag{2.29}$$

where $t_{off}^i \approx i t_{off} \exp \frac{(i-1)E_b}{k_B T}$.

In case of i parallel bonds that break cooperatively the dissociation rate is given by [20]

$$k_d^i = \frac{\exp -\tilde{f}}{t_{off}^i}. \tag{2.30}$$

When i parallel bonds break randomly [20],

$$k_d^i = \frac{1}{t_{off} \sum_{n=1}^{i} \frac{1}{n} \exp \frac{-\tilde{f}}{n}}. \tag{2.31}$$

When i parallel bonds break like a zipper (i.e. every time one bond experiences the full force, when this bond breaks the next bond feels the force) [20],

$$k_d^i = \frac{1}{t_{off} \sum_{n=1}^{i} n \exp -\tilde{f}}. \tag{2.32}$$

When i bonds in series break randomly the attachment ceases to exist when one bond breaks and [20]

$$k_d^i = i \cdot k_d^1. \tag{2.33}$$

The dissociation curve that would be measured in case an ensemble of beads is monitored in which not all beads are bound with the same number of bonds is described by:

$$S_1^* = \sum_i \eta_i \exp -k_d^i(f)t, \tag{2.34}$$

where S_1^* is the fraction of beads in de bound state, i is the number of bonds per bead, η_i is the fraction of beads bound with i bonds and $k_d^i(f)$ is the force dependent dissociation rate constant corresponding to an i bond attachment. Thus if the dissociation of beads with different numbers of bonds is measured higher order exponential behavior will show up in the dissociation curves. How the different exponents relate to each other at a certain force depends on the configuration of the bonds.

Chapter 3

Materials and Methods

To be able to apply forces to the Biotin - Streptavidin and Biotin - Anti-Biotin bond, the molecules are immobilized on a surface. A flat substrate is activated with Biotin. Streptavidin and Anti-Biotin are immobilized on the surface of superparamagnetic beads. After the bead and surfaces are activated they are brought in a setup where the actual experiment takes place. The setup consists of three parts: a sample holder to support the substrate and to incubate the beads in, a microscope system to observe the beads bound to the substrate and a magnetic system to apply a force to the beads. This force can either be a constant force or a force that is steadily increased in time for DFS experiments. An overview of the total setup is given in figure 3.1. The various aspects of this setup are addressed in this chapter.

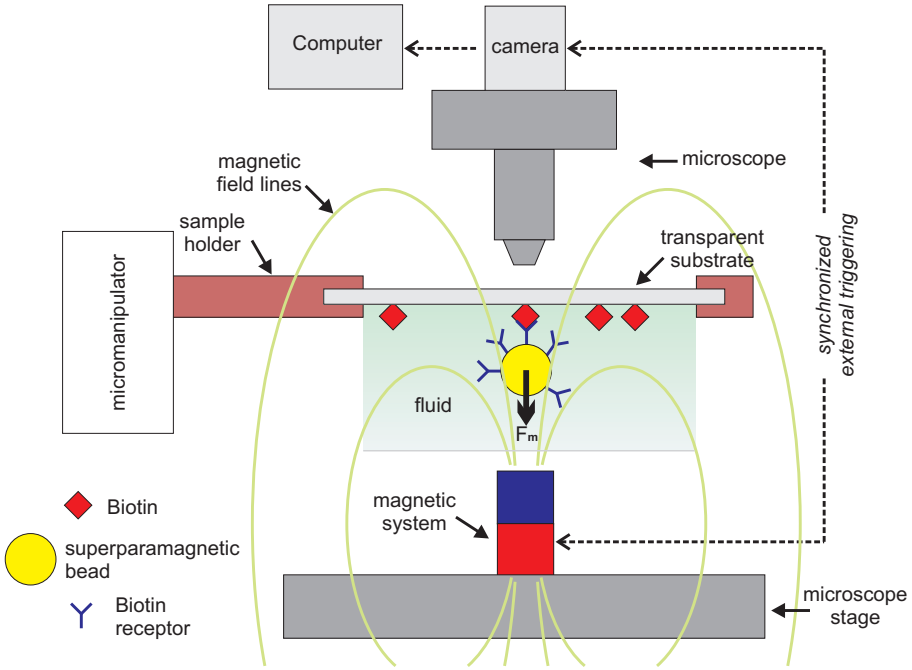

Figure 3.1: Overview of the total experimental setup. Figure not to scale.

3.1 Requirements and constraints

The dissociation of a single molecular bond can best be measured if the a bead is bound to the surface by only one specific molecular bond. Furthermore this bead, bound by a molecular bond, should be distinguishable from a bead that is bound via non-specific interactions between the bead and surface. Therefore the bond strength of non-specifically bound beads, if they are present, should be either much lower or much higher than that of specifically bound beads. In the best case the number of non-specifically bound beads is zero or at least low compared the number of specifically bound beads.

To enable the study of dissociation of the Biotin-Streptavidin bond on a timescale of minutes, forces in the range of 10-100 pN need to be applied to the bond. To be in the constant force regime these forces must be applied instantaneously. Furthermore, the statistic nature of bondbreaking events demands that many beads are monitored. The bondbreaking experiments should thus either be easy to repeat many times, or the same force should be applied to a lot of beads that are monitored simultaneously. The last is the most time efficient. In perspective of the research described here this demand can be formulated as: the force has to be constant over the area in

which the beads are monitored.

Figure 3.2: The Leica DM6000M microscope.

Dimensional constraints for the rest of the setup are given by the dimensions and the working distance of the microscope system that is used. The microscope is depicted in figure 3.2. The working distance for the used objective on the microscope is 2.2 mm. Since the microscope is a non-inverted one, the bound beads will have to be observed from above. The magnetic system should thus be very small to be able to pull of beads that are on top of a substrate without blocking the view. That is why a different approach is chosen. Beads are incubated at the bottom of a transparent substrate so that beads can be observed through it, and the force can be applied from below. In this case the distance from the objective to the bottom of the microscope stage limits the size of the magnetic system.

3.2 Activation of the substrate

3.2.1 Buffer solution

When experiments are done with proteins they are usually contained in a buffer solution as the environment of a protein is very important for its functionality. A buffer solution is a solution that can resist small changes in the pH when it is diluted or a certain amount of acid or base is added. The buffer that is used in this project is Phosphate Buffered Saline (PBS) which consists of salts: 137 mM NaCl and 2.7mM KCl and for the buffering functionality: 8 mM Na_2HPO_4 and 2 mM KH_2PO_4 in ultra pure water. The pH of this buffer is 7.4 which is approximately the pH of blood. The salts in this buffer have a shielding effect on the (surface) charges of molecules and on surfaces in (contact with) the solution.

To create an even more stable environment for proteins like antibodies, Bovine Serum Albumin (BSA) can be added to the buffer solution. Serum albumin is the most abundant protein in blood plasma. BSA is serum albumin derived from cow blood. In the blood it helps maintaining osmotic pressure. BSA has the shape of a prolate spheroid with a short axis of about 4 nm and a long axis of about 14 nm. At a neutral pH it has a net charge of -17 e per molecule and a molecular weight of 66.5 kg/Mole [34]. BSA can also be used to coat a surface with, in order to prevent the adsorption of other proteins to that surface. This process is called blocking.

When a buffer solution is used to bind proteins to a surface a surfactant can be added to prevent non-specific binding of proteins. The surfactant can also help washing away unbound proteins. A surfactant is a molecule that

has both hydrophilic and hydrophobic groups. Therefore it can bind to a hydrophobic surface and still be solved in water. When the surfactant binds to a hydrophobic part of a protein it prevents interaction of this molecule via non-specific hydrophobic interactions with the surface or other molecules. In this project Tween20 is used as a surfactant.

3.2.2 Principle of activation

Biotin has been coupled to a transparent polystyrene substrate via adsorption of BSA. Commercially available BSA with Biotin coupled to it (Biotin-BSA)(Pierce, #29130) is used. Each Biotin-BSA molecule has 8-12 Biotin molecules attached to it. This is not favorable for single bond dissociation experiments, as multiple bonds can form between one Biotin-BSA molecule and a Streptavidin coated bead. The possibility that beads can bind to multiple Biotin molecules on Biotin-BSA is taken into account in the analysis of the experimental results. The probability that bonds will form between a bead and Biotin molecules from different BSA molecules is minimized by adsorbing Biotin-BSA that is diluted with BSA in a PBS solution. The density of Biotin-BSA molecules on the surface is thus lowered because a large part of the surface gets covered by BSA molecules without Biotin.

BSA was found to adsorb stronger to hydrophobic polystyrene than to hydrophillic polystyrene [35]. The polystyrene used here is obtained from transparent Phoenix Biomedical injection molded petri dishes and is hydrophobic. After coating with BSA the surface is hydrophillic as the BSA molecules directs its hydrophobic parts to the substrate and its hydrophillic parts towards the aqueous buffer.

The bond between BSA and polystyrene should be much stronger than the bond between Biotin and its receptor to ensure that the first bond that breaks when a force is applied is the ligand - receptor bond. There are studies that investigate the strength of the bond between BSA and hydrophobic polystyrene [36] but it turns out to be hard to quantify this for a single BSA molecule. Another study shows that BSA bound to polystyrene does not come off in 50 hours [37]. This would mean that the bond indeed is stronger than the Biotin-Streptavidin bond.

The concentration of Biotin-BSA that is used in most experiments is 0.4 μg/ml in a 1 mg/ml BSA solution. In a very rough approximation this would yield one Biotin-BSA molecule per $14 \cdot 10^4$ nm^2. In this approximation Biotin-BSA and BSA are assumed to adsorb in the same extend to the polystyrene and the surface is assumed to be densely packed with (Biotin-)BSA molecules. If a superparamagnetic bead is assumed to be a sphere with a radius of 2.8 μm and the distance over which the two surfaces can interact is taken 10 nm than the total surface area available for interaction would be $9 \cdot 10^4$ nm^2. In this area expectedly there is no or one Biotin-BSA molecule available to interact with, if Biotin-BSA is distributed uniformly

over the surface.

3.2.3 Procedure and variations

The procedure for preparing a BSA or Biotin-BSA coated substrate is stated in the list below. The items marked with letters give the possible variations for a process step. Step 3 is the key step in this process, here BSA or a mixture of BSA and Biotin-BSA is adsorbing to the surface. Surfaces with only BSA are produced as controls and to investigate non-specific binding. Step 5 is an optional blocking process with BSA after the initial adsorption which is included to minimize non-specific binding. The amount of non-specific binding of beads to the surface is strongly dependent on which variant is chosen for each process step.

1. Cut substrates
2. Clean substrates in Isopropanol in ultra sonic bath for 1 minute, blow dry with Nitrogen
3. Overnight incubation
   (a) in 1mg/ml BSA in PBS
   (b) in 0.04% Biotin-BSA in 1mg/ml BSA in PBS
4. Wash substrates
   (a) in PBS with 0.05 % Tween20
   (b) in PBS
5. Block in 10mg/ml BSA in PBS for 1 hour
6. Wash substrates
   (a) in PBS with 0.05 % Tween20
   (b) in PBS
   (c) in ultra pure water
7. Keep substrates
   (a) in 10mg/ml BSA in PBS
   (b) in PBS with 0.05 % Tween20
   (c) blow dry with Nitrogen

3.2.4 Characterization

The lowest amount of non-specific binding is obtained if no Tween20 is used and when after the blocking step the surfaces are rinsed in ultra pure water and blown dry. Surfaces coated with BSA this way, have been characterized by AFM. Also a bare polystyrene surface has been imaged to see the initial surface roughness. The results are shown in figure 3.3. On the bare polystyrene scratch-like roughnesses with a hight in the order of magnitude of 10 nm are observed. The height profiles, taken in the area outside the scratches, depicted in figure 3.3(a) show that outside these scratches the surface has only a roughness of about 1 nm. The image of the BSA coated surface in figure 3.3(b) shows globular features with a hight between 2 and 7 nm that can be associated with BSA molecules. The width of some of the features is between 20 and 50 nm, which is larger than the size of one BSA molecule. Possibly small BSA clusters are observed.

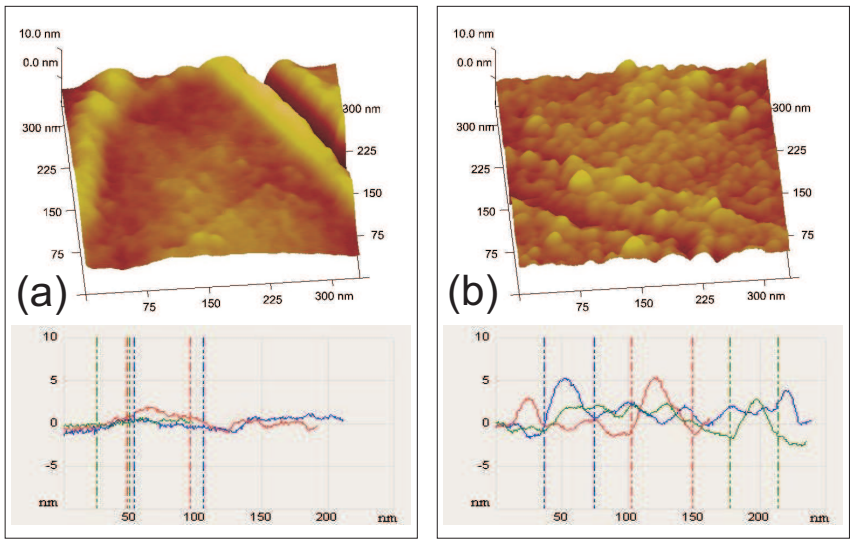

Figure 3.3: AFM image and height profile of (a) a bare polystyrene surface (b) a polystyrene surface with BSA adsorbed on it. The three colors in the height profile match three different sections.

3.3 Superparamagnetic beads

The superparamagnetic beads used in this project are polystyrene spheres with small Magnetite (Fe_2O_3) grains in it, as schematically depicted in figure 3.4. Bulk Fe_2O_3 would behave ferrimagnetic and would thus have a large magnetization at room temperature, also when there is no external magnetic field present. The time averaged magnetization of the grains in the

beads however is in general zero at zero field. This is because the volume of these grains is so small that the energy needed to change the direction of the magnetization of the entire grain is small compared to the thermal energy. The size of the grains is about 6-12 nm [38]. The thermal energy is sufficient to randomize the direction of the magnetization in the grains. Superparamagnetic beads placed in a magnetic field do get magnetized, and magnetic forces can be applied to the beads. For a more extensive description of superparamagnetism and other types of magnetism see reference [2].

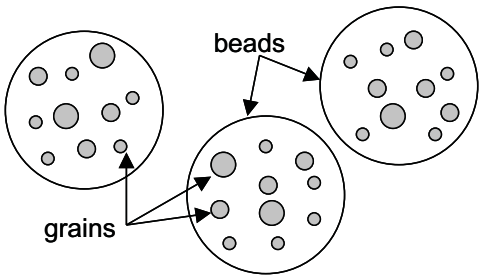

Figure 3.4: Schematic representation of superparamagnetic beads [39].

In the following section, 3.3.1, expressions are derived for the force on such a bead due to an externally applied magnetic field. In section 3.3.2 the properties of the beads used in this project are described. Section 3.3.3 concerns the forces that magnetized beads experience because of neighboring beads.

3.3.1 Bead actuation

The magnetic induction $\mathbf{B}$ $[T]$, the magnetic field strength $\mathbf{H}$ $[Am^{-1}]$ and the magnetization $\mathbf{M}$ $[Am^{-1}]$ of an object placed in a magnetic field are related via:

$$\mathbf{B} = \mu_0(\mathbf{H} + \mathbf{M}), \tag{3.1}$$

where μ_0 is the permeability of free space, given by $4\pi \cdot 10^{-7}$ $[Tm/A]$. The magnetization is defined as the magnetic moment of an object divided by its volume, $\mathbf{M} = \frac{\mathbf{m}}{V}$. To what extent an object magnetizes in the presence of an external applied field $\mathbf{H}$ is given by the magnetic susceptibility χ, for low values of $\mathbf{H}$ the following relation is valid:

$$\mathbf{M} = \chi\mathbf{H}. \tag{3.2}$$

Above a certain value of $\mathbf{H}$, saturation occurs. This means the magnetization of the object increases more slowly with the magnetic field at higher

fields and finally approaches a constant value, the saturation magnetization M_{sat}.

The magnetic force $\mathbf{F_m}$ $[N]$ on a magnetized object is given by:

$$\mathbf{F_m} = \mu_0 \int_V (\mathbf{M} \cdot \nabla)\mathbf{H}\, dr^3, \tag{3.3}$$

where V is the volume of the object and $\mathbf{H}$ the magnetic field strength in the absence of the object. Under the assumption that the magnetic field gradient is constant over the volume of the object this expression simplifies to:

$$\mathbf{F_m} = \mu_0 V(\mathbf{M} \cdot \nabla)\mathbf{H}. \tag{3.4}$$

Substituting equation 3.2 and using $\mathbf{B} = \mu_0\mathbf{H}$, which is valid if the object is surrounded by a medium with $\chi = 0$, the magnetic force on the object can be obtained:

$$\mathbf{F_m} = V\chi\nabla\left(\frac{\mathbf{B}^2}{2\mu_0}\right). \tag{3.5}$$

This expression is only valid when the magnetic moment in the object is not saturated. In the case of saturation instead of equation 3.2, $\mathbf{M} = M_{sat}\frac{\mathbf{H}}{|\mathbf{H}|}$ should be used, leading to:

$$\mathbf{F_m} = \frac{VM_{sat}}{2|\mathbf{B}|}\nabla\mathbf{B}^2 = m_{sat}\nabla|\mathbf{B}|, \tag{3.6}$$

where m_{sat} $[Am^2]$ is the saturation magnetic moment.

3.3.2 Bead properties

The beads used in the majority of bond strength measurements are the Dynal Dynabeads® M-270. These beads have a mean diameter of 2.8 μm, a saturation magnetic moment of $m_{sat} = 1.73 \cdot 10^{-13} Am^2$, and a characteristic bead density of ρ =1.4·10^3 kg/m^3.[38] The resultant of gravitational and buoyancy forces on a bead dispersed in a watery fluid can be found using the following expression:

$$\mathbf{F_g} = V(\rho - \rho_{fluid})\mathbf{g} \tag{3.7}$$

where ρ_{fluid} is the density of the fluid and V is the volume of the bead. For a bead density of ρ =1.4·10^3 kg/m^3, and taking ρ_{fluid} =1.0·10^3 kg/m^3 the density of water and a bead volume of $V = 1.15 \cdot 10^{-17} m^3$, this force is 45 fN. This gravitational force is small compared to the forces needed to break a specific molecular bond. Nevertheless it is sufficient to make the beads sediment, beads do not stay in solution if they are not stirred. This property of the beads is used to incubate the beads on an activated surface.

Some experiments have been performed with smaller beads, the Dynal Dynabeads® MyOne^{TM} T1. These beads have a mean diameter of 1 μm, a

saturation magnetic moment of $m_{sat} = 2.09 \cdot 10^{-14} Am^2$, and a characteristic bead density of ρ =1.7·10^3 kg/m^3.[38] The gravitational force on this type of beads in a aqueous solution is 1.14 fN.

The saturation magnetic moment of the beads mentioned in the previous two paragraphs are mean values. Bead to bead variations in saturation magnetic moment are expected as the quantity of magnetic material in the beads is not necessarily equal in every bead. The variation in saturation magnetic moment is estimated to be 10% at most.

For the different experiments beads have been used with two different coatings. For the experiments on the Biotin - Streptavidin system Streptavidin coated M-270 and MyOne^{TM} T1 have been purchased form Dynal. Although the coating of these beads is the same, they have slightly different surface properties because the surface before coating is different. While the M-270 bead surface before coating contains carboxylic acid (-COOH) head groups, the MyOne^{TM} T1 bead surface before coaction contains tosyl (p-toluenesulfonate) head groups. The isoelectric point of the Streptavidin coated M-270 beads (the pH at which it has no net surface charge) is at a pH of 4.5 whereas it is at a pH of 5 for the MyOne^{TM} T1 beads. Further the surface of the M-270 beads is more hydrophillic (contact angle with water is 60^o) than the surface of the MyOne^{TM} T1 beads (contact angle with water is 80^o)[40]. In figure 3.5 an AFM image of an M-270 Streptavidin coated bead is shown that is taken in fluid. From SEM images, recorded in vacuum, it was already known that the beads were not nice round spheres but had a lot of protrusions. In the fluid AFM, where the bead is kept under conditions more similar to the normal working conditions, the same irregular surface shows up.

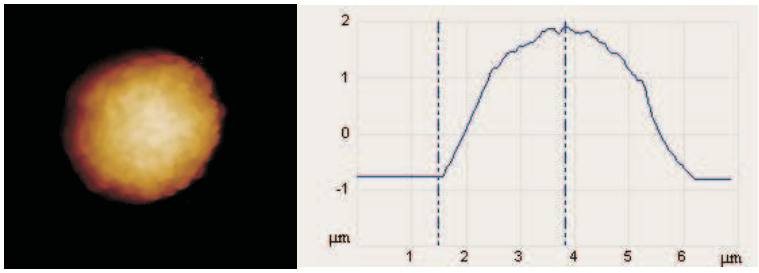

Figure 3.5: AFM image and hight profile of a M-270 Streptavidin coated bead recorded in fluid.

For the experiments on the Biotin - Anti-Biotin system M-270 beads with carboxylic acid (-COOH) head groups are used as a starting point. To these head groups goat Anti-Biotin (Pierce, #31852) is covalently coupled via an EDC coupling reaction. EDC, short for 1-ethyl-3-(3-dimethylaminopropyl) carbodiimide hydrochloride, activates the carboxylic acid head groups on

the beads, so that they can react with amino groups (-NH_2) on the Anti-Biotin to form amide bonds. A detailed protocol for this coupling reaction is given in appendix [A].

Before the beads are used in experiments they are washed and diluted in a buffer solution. The final concentration of beads is about 10^8-10^9 beads per milliliter.

3.3.3 Interaction between beads

Superparamagnetic beads in an externally applied magnetic field will get magnetized. When there is a gradient in the externally applied field, a force will be exerted on the beads in the direction of the field gradient (equations 3.5 and 3.6). If two of the magnetized beads are close to each other, and the gradient of the magnetic field of one bead at the position of the other bead is large, an extra force is exerted on the beads as a consequence. In experiments assessing force dependent dissociation it is important for sensitivity that the direction and magnitude of the force on the beads is the same for all beads. Therefore the forces on the beads have been calculated for two beads that are in a large externally applied field and in saturation. The magnetization is assumed to be directed in the direction of the externally applied field as this is large in comparison to the field induced by the beads. The beads are modeled to be point dipoles with the saturation magnetization of an M270 bead and the external field is directed along the negative z axis. In figure 3.6 the direction of the force that a point dipole would feel in this situation is plotted.

Demanding that at z = 0 the force on one bead in the x direction, induced by a neighboring bead, should be smaller than 10% of the force applied via the external field, a minimum separation distance of the beads can be derived. This minimum separation distance depends on the magnitude of the externally applied force. For a force of 10 pN the separation between the centers of two beads should be about 9 μm, for a force of 40 pN the separation between the centers of two beads should be about 6.5 μm, for higher external forces the beads can be closer. In the analysis of experimental results beads that are too close to each other should not be taken into account.

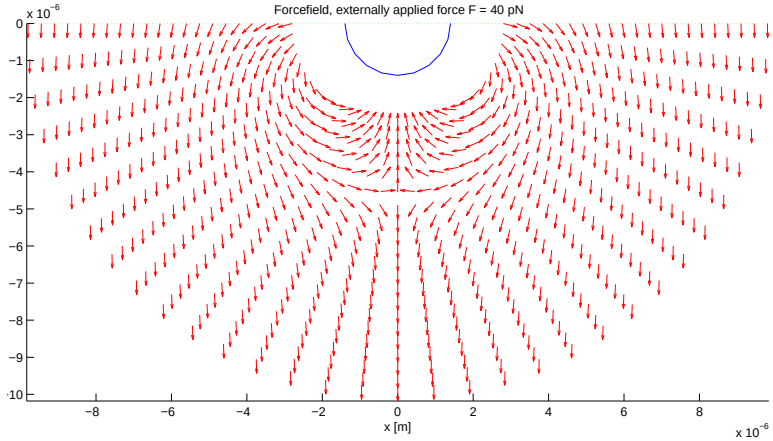

Figure 3.6: Direction of the force exerted on a point dipole with a magnetization in the negative z direction by a magnetized bead on a fixed position (indicated by the blue line) and an external magnetic field directed in the negative z direction.

3.4 Sample holder

The sample holder as depicted in figure 3.7 is made out of brass and is attached to a micromanipulator. By operating the micromanipulator, the height and position of the sample holder can be accurately adjusted. The sample holder contains a small fluid compartment of about $400\mu m$ high and 6 mm in diameter. Over this fluid compartment the activated polystyrene slide can be mounted. The compartment is shallow to enable the magnetic system to approach the activated surface very close. The bottom of the compartment is reflective to maximize the quantity of light that is reflected back into the microscope, this improves the contrast of the image. It consist of a glass microscope slide with a thin layer of gold sputtered on it. This slide is fixed by a ring and 2 screws and can be replaced if needed.

After the polystyrene is mounted over the fluid compartment with its activated side at the bottom, beads can be incubated at the activated surface. A suspension of beads in a buffer can be injected via a small inlet into the fluid compartment. The incubation is done by turning the sample holder upside down and letting the beads sediment for a certain incubation time. After incubation the sample holder is turned back and placed under the microscope. After the microscope is focussed on the beads bound to the polystyrene the magnetic system is positioned under the sample holder by adjusting the microscope stage.

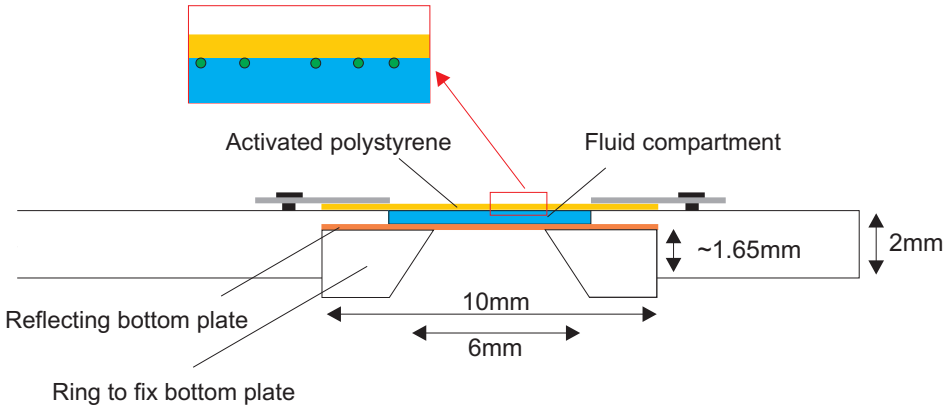

Figure 3.7: Side view of the sample holder

3.5 Optical detection

3.5.1 Microscope and camera

For optical detection of beads, a Leica DM6000M microscope is used. On the microscope five objectives are present. In this project the beads are observed through a droplet of water on the polystyrene, using an immersion objective with a magnification of 63 times. The ocular gives an additional magnification of 10 times resulting in a total magnification of 630 times. Images are recorded with a Redlake MotionPro HS-3 high speed camera, which is mounted on top of the microscope. It records grayscale images with a maximum resolution of 1280×1024 pixels. At a magnification of 630 times a 1280×1024 pixel image corresponds to an area of 185×230 μm. The camera is operated via a computer, on which the data is also stored. For force induced dissociation experiments the camera is triggered externally and synchronized with the magnetic system. The power supply of the magnetic system (Agilent Technologies E3631A Triple Output DC Power Supply) is connected with its 25V output to the magnetic system and with its 6V output to the external trigger input of a function generator. This function generator is preprogrammed with a function of block pulses. The output of the function generator is connected to the camera, at each up going flank of a block pulse the camera records an image. In the first second images are recorded at a frequency of 10 Hz in the next 9 seconds images are recorded at 5 Hz and after that at 1 Hz. The first image is recorded 50 ms after the power supply is turned on in the case of constant force experiments. In the case of DFS experiments the voltage on the magnetic system is increased in steps. In this case the first image is recorded 60 ms before the first incremental step in voltage.

3.5.2 Bead counting software

A typical output of an experiment is a series of images that show the beads that are bound to the polystyrene at different times after the force is switched on. To count the beads in each frame manually is very time consuming therefore bead counting software has been developed. The used script can be found in Appendix [B]. The software needs the coordinates of the beads in the first image as an input. The user can give this input by mouse clicks on the first image. For each subsequent image it records the intensities of pixels around these coordinates. If the cumulative change in intensity around a coordinate between two successive frames is higher than a threshold value, this means a bead has disappeared. The program gives the number of beads that is still left in each frame as an output.

3.6 Magnetic system

3.6.1 Design

To exert magnetic forces of 10-100pN on a small superparamagnetic bead, very high field gradients should be generated. Substituting the saturation magnetization of an M270 bead in equation 3.6 shows that $\nabla|\mathbf{B}|$ should be up to $600T/m$. These gradients have been generated in various ways, for example by a thin current wire very close to the bead [26], by a (electro-) magnetic microneedle [41] or by a permanent magnet [30]. Electromagnets have the advantage that they are switchable, however it is not easy to reach high field gradients over larger distances with small electromagnets. With the current wire and micro needle high gradients are achieved because they are operated very close ($\sim 10\mu m$) to the beads. The disadvantage of this is that the force depends strongly on the position of the bead and is only applied to the one or few beads that is/are close enough. With a strong permanent magnet further away (a few mm) from the beads, it is easier to have gradients that are large and constant over a larger area, however to apply an (almost) instantaneous force with a permanent magnet is difficult as it will have to be moved very fast and accurate. That is why in this project a relatively big electromagnet is used that can approach the surface with beads up to 500 μm. The magnet is situated on the microscope stage, the height of this stage can be adjusted with micrometer accuracy.

The magnetic system consists of a Copper wire coil with a Soft Iron core. See figure 3.8 for a schematic representation of the system and for dimensions. The core has a tip that is flattened off, the diameter of the flat area being 1 mm. The tip has the function of guiding the magnetic field trough an area that is getting smaller towards the point in order to create a large gradient just above the core tip. The tip is flattened off to create an area above the tip over which the magnetic field gradient is constant. In this

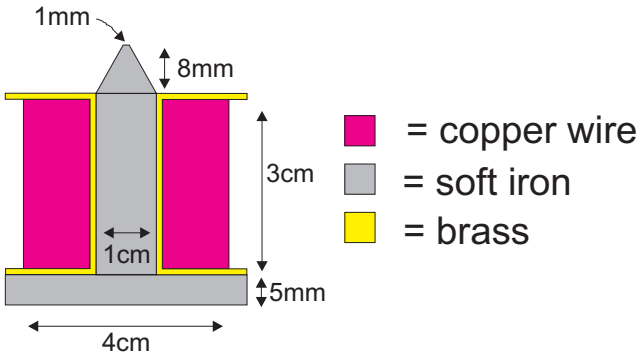

Figure 3.8: Schematic representation of the magnetic system.

area the force exerted on all similar beads is the same. The Copper wire coil is wound on a brass holder that can be taken of the core. The core is coated with a thin layer of Nickel to prevent the Soft Iron from oxidizing. The coil consists of Copper wire with a diameter of 0.38 mm and has an inner diameter of 12 mm and an outer diameter of 23 mm. At room temperature it has a resistance of 22.5 Ω.

During experiments the maximum current that is sent through the coil is 1 A. At this current a lot of heat is generated in the coil. To prevent the coil from melting and to enable continuous operation a cooling system is used. The coil is put in a water container with a water inlet and outlet. Using a small pump connected to the container by silicon hoses, water is pumped around at a speed of about 10 l/hr. The silicon hose is led through a large reservoir of cold water to improve heat exchange. With the cooling system in operation, the internal temperature of the coil stays below 45 ^{o}C.

To apply higher forces to beads, higher currents could be used. These can be obtained using a more powerful power supply than has been used here. The maximum current is determined by the heating of the coil.

In the case of DFS experiments the voltage on the magnetic system is increased in steps. The voltage increment per step depends on which loading rate is to be applied. As an approximation a linear relation between the current trough the coil and the applied force is assumed. The range of loading rates that can be obtained in the present setup is limited by the power supply. The output of this power supply can only be increased every 60ms. Using a power supply of which the output can be increased continuously or at a higher rate, it is possible to obtain higher loading rates.

3.6.2 Comsol simulation

The magnetic induction of the coil and core described in the previous section have been simulated using the software package Comsol Multiphysics.

A surface and field line plot of this induction is given in figure 3.9. The simulation is done in 2D to simplify calculations, as the axial symmetry of the system allows the 2D solution to be extrapolated to 3D.

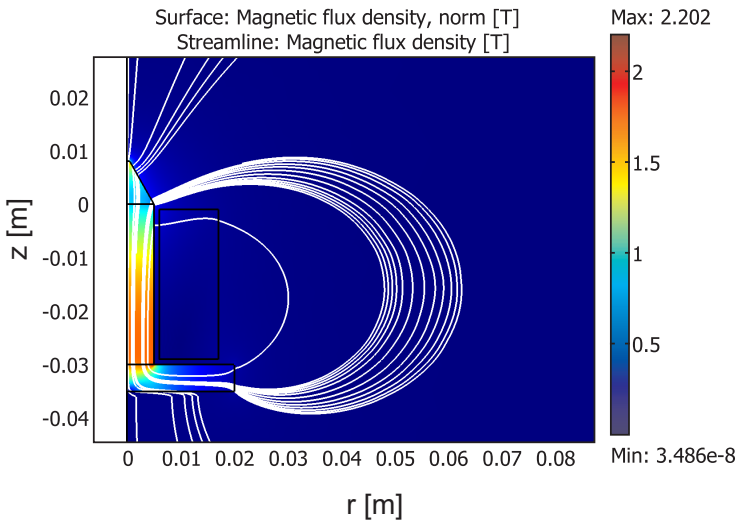

Figure 3.9: Comsol simulation of the magnetic induction around the coil.

The magnetic induction at a distance of 500 μm above the core tip is about 0.5 T when a current of 1 A is sent through the coil. Beads at this distance will be magnetized to their saturation magnetization. Making use of equation 3.6 and the simulated magnetic induction, the force that can be exerted on M270 beads has been calculated for different current densities in the coil as a function of the distance above the core tip. The result of this calculation is shown in figure 3.10.

In case a current of 1 A is sent through the coil, forces between 80 and 90 pN are exerted on the beads in the working range of the setup. At a current of 100 mA the force on beads at the same distance is only 10 pN. At an intermediate current of 500 mA forces between 45 and 50 pN are exerted. These forces are in the right range to study the Biotin-Streptavidin bond. It is possible to apply up to 20% higher forces with the developed magnetic system by using a smaller distance between the beads and the magnet as has been done in this project.

The force exerted on beads has also been calculated as a function of the radial distance from the center of the coil. In figure 3.11 this force is plotted for two different distances above the core tip in the working range of the setup. The variations in force given in figure 3.11 correspond to variations over a circle shaped area of 67500 μm^2 around the center of the coil. This

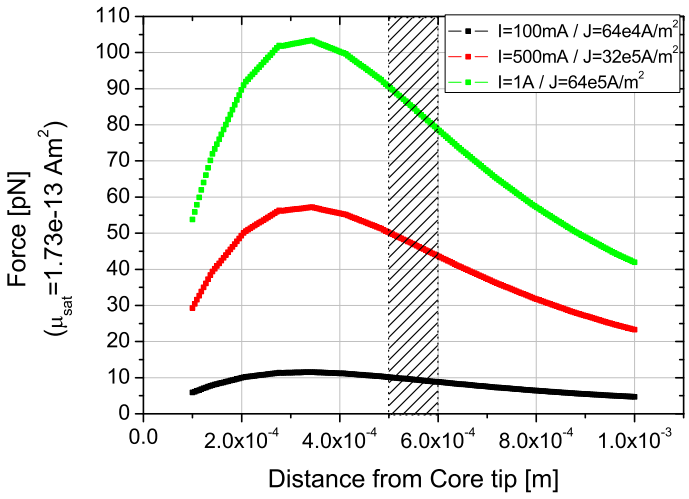

Figure 3.10: Calculated force exerted on a M270 bead as a function of the distance from the core tip for three different currents through the coil. The dashed area marks the working distance when the magnetic system is used in combination with the sample holder.

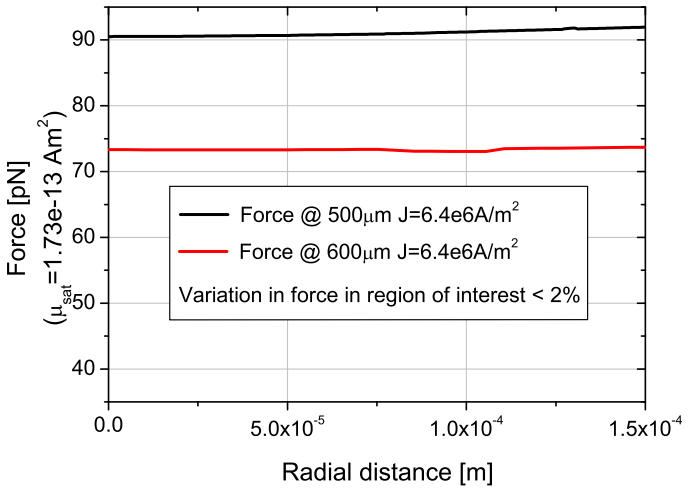

Figure 3.11: Calculated force exerted on a M270 bead at 500 and 600 μm above the core tip, as a function of the radial distance from the center of the coil.

area overlaps the area that is imaged by the camera at a magnification of 630 times. Depending on the exact height above the core tip the maximum variation in force on beads with the same saturation magnetization is 2 % at most.

3.6.3 Characterization

The system is first characterized by probing the magnetic induction above the center of the core tip, using a Hall probe (F.W. Bell model 5070 Gauss/ Tesla meter). This probe is a long rectangular slab with a thickness off about 1 mm. It contains an active sensor area of 0.4 mm in diameter at the tip that registers the magnetic induction perpendicular to the slab. The active area of the probe is positioned above the center of the core tip. Due to the thickness of the probe, the center of the probe can only approach the core tip up to 0.5 mm and the sensor readout is actually an average of the magnetic induction around this value. The magnetic induction is measured as a function of the distance above the core tip for two different currents trough the coil. The results are given in figure 3.12, together with the results of the Comsol simulation.

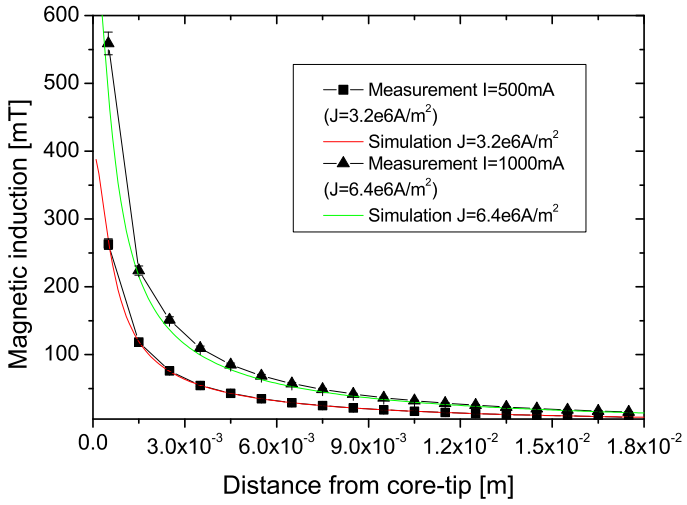

Figure 3.12: Magnetic induction in the z direction measured with a Hall probe, as a function of the distance above the core tip for two different currents trough the coil. The red and green lines represent the results of the Comsol simulation at the corresponding current densities.

From figure 3.12 can be concluded that the behavior of the actual coil is consistent with the simulated behavior in the measured range. However

the working distance of the coil system will be around 500 μm above the coil tip. In the range around 500 μm there is only one measurement point that gives an average of the magnetic induction. This is insufficient to prove directly that the real coil will show the simulated behavior in this range, nevertheless the overall match of the curves gives an indication that the simulation is trustworthy and can be used to estimate the force applied to a bead in the working range of the coil.

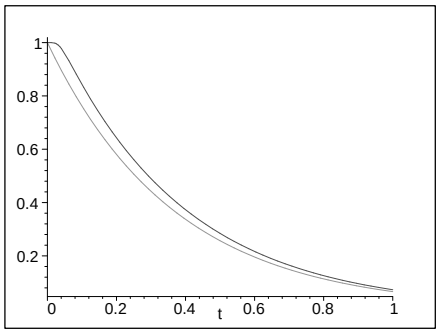

(a) $F = 100pN$

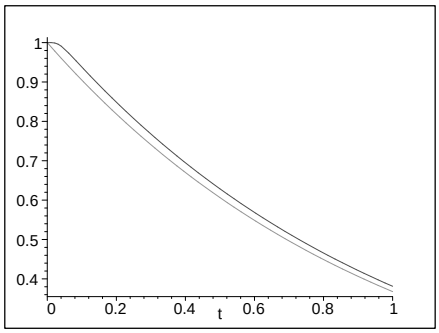

(b) $F = 90pN$

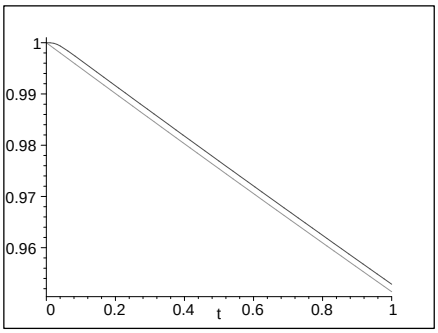

(c) $F = 60pN$

Figure 3.13: Probability to be in the bound state as a function of time (t [s]) for different applied forces. The lower curve is behavior when the force is applied instantaneous, the upper curve is for force application with an RL-time of 13 ms.

The system is also characterized by its RL-time, τ. The RL-time is measured to be 13 ms. Making use of literature values for t_{off} and x_β for the Biotin-Streptavidin system, the effect of the force not being instantaneous in constant force measurements is investigated. This is done by solving equation 2.25. The dimensionless loading rate corresponding to an LR-system taken for $\tilde{r_f}$. This loading rate is derived, assuming a linear relation

between the current trough the coil and the applied force.

$$\tilde{r_f} = \frac{t_{off}}{\tau} \cdot (\tilde{f_s} - \tilde{f}), \tag{3.8}$$

were $\tilde{f_s}$ is the dimensionless force when $t \to \infty$ and $\tilde{f}$ is the dimensionless force at time t which is given by:

$$\tilde{f} = \tilde{f_s}(1 - \exp(\frac{-t}{\tau})) \tag{3.9}$$

In figure 3.13 the calculated probability to be in the bound state, S_1, is given as a function of time for different applied forces. In each graph both the results for a time independent, instantaneous, force and a time dependent force corresponding with an RL-system with $\tau = 13ms$ are plotted. It turns out that the effect of the time dependance in the force is that the decay of S_1 in time is not really exponential, it starts a little later but approaches exponential behavior again after a few seconds. This effect is most pronounced at high forces. At 100 pN the values for S_1 deviate up to approximately 10 % in the initial phase. At 90 pN the deviation is only 2 % and at 60 pN it is negligible. Because at high forces the initial phase of the decay is especially important the error caused by applying a non instantaneous force, that is already large in this regime, weighs heavy in the final value of k_d. In this project measurements have been done at forces up to 90 pN. In this regime the error in k_d caused by the force not being instantaneous is 2 % at most.

3.6.4 Force accuracy

There is a number of factors that determine the accuracy with which the force on the beads can be applied and determined:

- There are variations ($< 2\%$) in the magnetic field gradient over the surface region of interest.
- The saturation magnetization varies ($< 10\%$) between beads.
- The separation distance between the surface and the magnetic system is measured with an inaccuracy of 2-4%. This results in inaccuracies in the derived force of 1-3%.
- The force at the measured distance from the magnetic system is derived from simulation results.

There are thus bead to bead variations in the applied force which are estimated to be $< 12\%$. These variations can be lessened by using an isolated fraction of beads with the same saturation magnetization. The accuracy with which the mean force on the beads is known depends strongly on how

good the simulation results match the actual situation. Considering the results presented in 3.12, the mean force is estimated to be measured with an inaccuracy of less than 10%. For a better determination of the magnetic induction above the coil tip, measurements should be performed in the first millimeter above the tip with a smaller probe than described in section 3.6.3.

Chapter 4

The Biotin - Streptavidin model system

This chapter describes the results of measurements related to the Biotin - Streptavidin model system. In section 4.1 non-specific binding of Streptavidin coated beads on a BSA coated surface is addressed. In section 4.2 results of constant force experiments on the Biotin-Streptavidin bond are discussed. Finally, in section 4.3 extra attention is given to multiple bond attachments.

4.1 Non-specific binding

Unless non-specific binding is controlled, investigating specific bonds is not possible. The number of non-specifically bound beads should be low. Preferably such beads should detach quickly from the surface when only a small force is applied that does not affect specific bound beads to be able to make a distinction. A measure for the amount of beads attached to the surface via non-specific interactions, is the ratio between the number of beads bound to a plain BSA covered surface and the number of beads bound to a surface on which Biotin is present.

Measurements of non-specific binding of Streptavidin coated beads on a BSA coated polystyrene surface are presented in this section. The general setup of all these measurements is the same. First a polystyrene substrate covered with BSA is prepared. Beads coated with Streptavidin are washed and diluted in a buffer solution. Unless stated differently M-270 beads are used in all experiments. The BSA covered substrate is mounted in the sample holder, where the beads are incubated on the BSA for a certain incubation time. Finally the effect of applying a force to the beads is studied.

The process of preparation of the BSA covered substrates is subject to the variations described in section 3.2.3. The number of beads that initially bind (non-specifically) to the surface, N_0, is different for the different

preparation methods. Therefore the procedure that was used to prepare the substrate will be indicated for all measurements presented here.

4.1.1 Effect of buffer solution

Experiments presented in this section have been performed on substrates prepared by first washing polystyrene slides in isopropanol and drying them in a nitrogen flow. After that the slides are incubated overnight in a 1 mg/ml BSA solution in PBS. Next they are washed and stored in a PBS solution containing 0.05% Tween20.

The beads used in this experiment were contained in two different buffer solutions. The first consists of 0.05% Tween20 in PBS, the second contains an aditional 10 mg/ml BSA. Both buffers have a pH of 7.4. For an incubation time of the beads on the substrate of 30 s, N_0 is about 30 for both buffers.

In an ideal case the beads binding in a non-specific way are also beads that are weakly bound. In that case by applying a small force one would be able to remove all non-specifically bound beads from the surface while not or hardly affecting the beads bound specifically to the surface. When this is the case, a distinction can be made between specifically and non-specifically bound beads. To investigate whether indeed the non-specific bound beads are bound weakly, a small force is applied to the beads by sending a current of 100 mA, corresponding to a force of about 10 pN, through the coil.

In the graph presented in figure 4.1 the percentage of beads still present on the surface, is given as a function of time. N_0 is scaled to 100%, unless stated otherwise this is done for all similar experiments presented in the remainder of this report. It is observed that 70% of the beads incubated in the buffer containing BSA is removed in the 160 seconds that the force is applied, whereas less than 20% is removed in case the beads are incubated in a buffer without BSA. As in the last case many beads were still bound to the surface, a larger force was applied to these beads. This was done by sending a current of 1000 mA through the coil, corresponding to a force around 80 pN. In figure 4.1 also the result of this measurement is given. Here not N_0, but the number of beads that was left after applying a low force of 10pN for 160 s is scaled to 100%. It turns out that at this higher force 70% of the beads that were left after the first experiment now come of. However the remaining 30% resists a force of 80 pN for more than 2 minutes, indicating a very strong bond.

From the results presented in figure 4.1 it can be derived that non-specific bound beads are not necessarily weakly bound under the circumstances present in this experiment. Instead, the non-specific bonds seem to cover a range of strengths from very weak to very strong. This range overlaps with the expected range for specific bonds of 10-100 pN. The average strength of the non-specific bonds is lower when BSA is present in the buffer. There are several explanations for this observation. When beads

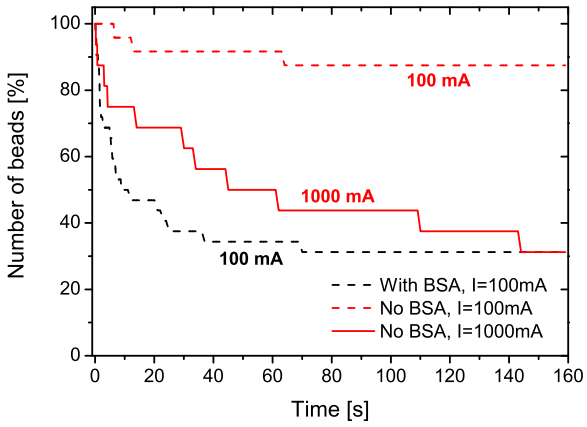

Figure 4.1: The effect of a force on Streptavidin coated beads bound on a BSA surface in different buffers.

are not entirely covered with Streptavidin or the polystyrene surface is not entirely covered with BSA, the empty spots might be occupied by BSA from the buffer. As BSA is negatively charged at a pH of 7.4 the adsorption of BSA to the beads and surface gives rise to an increase in the repulsive electrostatic interaction between the already negatively charged bead surface and BSA coated surface. Note that the average interaction is considered here whereas for the adsorption of BSA local interactions are important. Locally the hydrophobic interaction between BSA and the polystyrene or bead surface can be stronger than the electrostatic repulsion of the BSA. The fact that BSA covers locally hydrophobic surface areas also contributes to the reduction of non-specific binding. In all measurements presented in the remainder of this chapter the buffer of 10 mg/ml BSA in PBS with 0.05% Tween20 is used, unless stated otherwise.

An interesting observation has been done in an experiment were free Biotin in a concentration of 2 μM was added to a buffer consisting of 0.05% Tween20 in PBS. The free Biotin occupies a large fraction of the available Biotin binding sites on the Streptavidin coated bead. This is expressed in the lack of binding of these beads on a surface with Biotin-BSA. The binding on a surface with only BSA was not expected to be affected by the blocking of binding sites. However when these beads were incubated for 30 s on a BSA surface, N_0 was 2 where it was around 30 when no Biotin was added. The number of non-specifically bound beads has thus drastically decreased. This could be explained by the fact that Biotin gets folded in in the Streptavidin molecule as described in section 2.1.5 . The final folding of

a loop of amino acids over the Biotin in the binding pocket presumably has a stabilizing effect on the molecule, making it less favorable to interact with the surface.

4.1.2 Effect of bead size

Experiments presented in this section have been performed on substrates prepared by first washing polystyrene slides in isopropanol and drying them in a nitrogen flow. After that some of the slides (the blanks) are incubated overnight in a 1 mg/ml BSA solution in PBS. The others are incubated overnight in a 1 mg/ml BSA solution in PBS with 0.04% (i.e 0.4 μg/ml) Biotin-BSA added. On the blanks only non-specific binding can take place, on the slides with Biotin also specific binding can occur. After incubation all slides are washed in a PBS solution. Subsequently the slides are kept for one hour in a 10 mg/ml BSA solution in PBS as an extra blocking step. Finally they are rinsed in PBS and blow dried in a nitrogen flow.

From theory (equation 2.12) it is expected that if a sphere interacts with a surface via non-specific interactions, the force needed to detach it, is larger for a larger radius of the sphere. In this respect it thus could be worthwhile to use smaller beads if one wants to reduce non-specific binding. On the other hand, smaller beads usually also have a lower magnetic content so only smaller forces can be applied to them. In this experiment two sizes of Streptavidin coated beads are used, the M-270 beads having a diameter of 2.8 μm and the MyOne^{TM} T1 beads, having a diameter of 1 μm. As described in section 3.3.2 the surfaces of these beads are not completely the same. The MyOne^{TM} T1 surface is less negatively charged and more hydrophobic than the M-270 surface. These differences are largely compensated by the presence of BSA and Tween20, blocking the hydrophobic surface, and salts, shielding the charges, in the buffer solution. Nevertheless the outcomes of this experiment should be considered with some reservation.

The 2.8 μm beads have been incubated on the prepared substrates for 35 s, leading to a N_0 of $\sim$50 on the BSA surfaces and a N_0 between 50 and 100 on the Biotin-BSA surface. For the 1 μm beads the incubation time is increased to 60 s and a 2-10 times higher concentration of beads is used to compensate for the slower sedimentation of these beads. This leads to a N_0 of $\sim$15 on the BSA surfaces and a N_0 of $\sim$30 on the Biotin-BSA surface. These numbers, for both bead sizes, do not give a verdict on whether the bonds on the Biotin-BSA surface are specific, non-specific or a combination of the two. Therefore a 10 pN force is applied to the beads with a twofold purpose. In the first place to study the differences between the attachment forces for the two sizes of beads on a BSA surface. In the second place to see if it is possible, for this slightly altered process of surface actictivation, to remove the non-specifically bound beads from the Biotin-BSA surface while keeping the specifically bound beads.

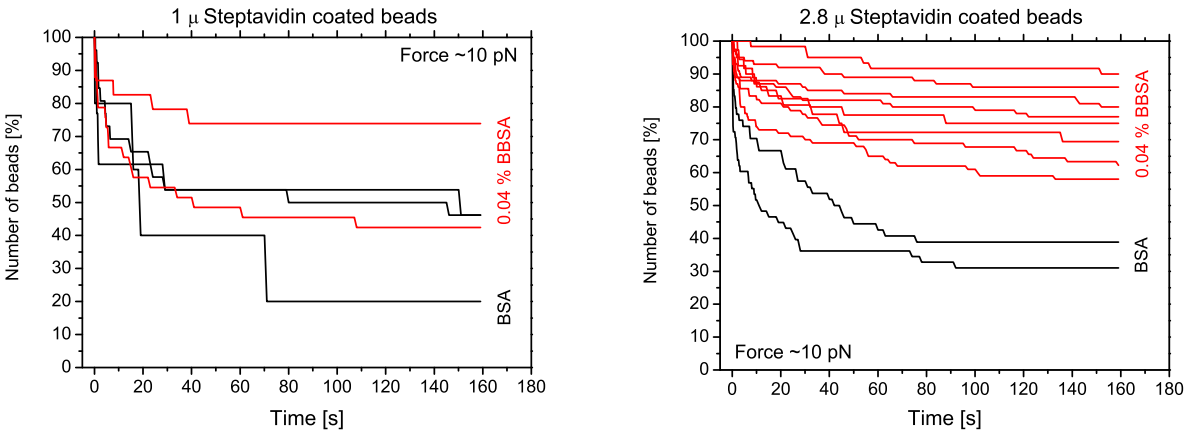

(a) (b)

Figure 4.2: Percentage of beads bound to the surface as a function of time at a force of 10pN. This is studied on beads with a radius of (a) 1 μm and (b) 2.8 μm on surfaces with BSA, black curves, and a mixture of Biotin-BSA and BSA, red curves.

In figure 4.2 the effect of a force of 10pN on the beads is depicted. First the case where there is only BSA present on the surface and were there are no specific bonds, is considered. In both figure 4.2(a) and 4.2(b) one can see that a considerable amount ($\sim 40\%$) of the beads resists the force for more than 160 s. Furthermore the shape of the decay curves is similar for the two sizes of beads. Although it was expected that the smaller beads would be pulled from the surface faster this does not follow from the measurements. An explanation can be that the formed non-specific bonds do not arise from the interaction of the total sphere with the surface but from interactions of either molecules or protrusions on the bead surface. However one would expect the number of molecules and protrusions in contact with the surface to be larger for larger beads, therefore the bond strength of larger beads would still be larger. Another possibility is that the difference in bond strength is not observed because of the difference in incubation time between the two sizes of beads.

The second issue to be considered is the specificity of the bonds on the surface covered with a mixture of BSA and Biotin-BSA. Figure 4.2 shows that in general less beads are removed from the surface with Biotin than from the BSA surface when a force of 10 pN is applied for 160 s. This is true for both bead sizes, however there is some overlap between the different surfaces in case of the 1 μm beads. The difference is not sufficient to be conclusive

about how many of the bound beads, that are still present on a surface with Biotin after 160 s of applying a force of 10pN, are specifically bound. For the beads that are left, each combination of multiple or single specific bonds and non-specific bonds is still possible. So neither based on initial numbers nor based on the effect of a small force on the beads can the definite nature of the bonds be determined in this experiment. Still, by applying a 10 pN force it is possible to discern between the two surfaces, indicating that at least some specific binding occurs on a surface containing Biotin-BSA.

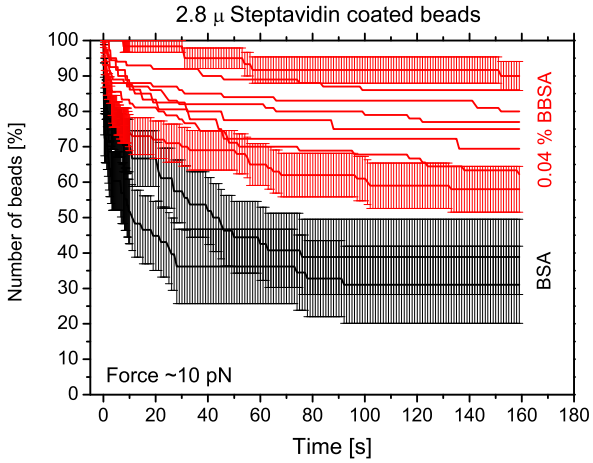

Figure 4.3: Dissociation curves from figure 4.2(b), with error bars for the expected statistical errors.

Maybe the most striking thing in this figure is that all black curves and all red curves in one graph are obtained under the same circumstances but do not yield the same result. The curves do however lie in a certain band depending on the type of substrate and beads. These bands are expected as the probability distribution for bond rupture is only probed by studying a limited number of bond breaking events.

There is a certain expectation value for the number of bonds that will break between time t and Δt. The probability that a certain number of bond breaking events will be observed in this time frame is governed by Poisson statistics as each bond breaking event is independent. The variance of the number of bonds breaking in each time frame is thus equal to the expectation value. The variance in the number of bond that is still present at a certain time, is derived by adding up the variances of the measured time frames up until that time. The absolute value of the standard deviation is given by the square root of the expectation value of the total number of bond breaking events up until a certain time. This number increases in time

and with the total number of bond breaking events studied. The relative value of the standard deviation with respect to the number of initially bound beads decreases with N_0. The percentage accuracy thus increases when a larger ensemble of beads studied.

In figure 4.3 error bars marking the standard deviation for the statistical errors are added to the curves from figure 4.2(b). These errors have been estimated by taking the observed number of bond breaking events in each time frame as the variance, because the expectation value is not known. The curves measured on a BSA surface are largely within each others margin of error. The curves measured on the Biotin-BSA show a much larger spread than would be expected from statistical variations. A possible cause for this is an inhomogeneous surface coverage of Biotin-BSA.

4.1.3 Constant forces on non-specific bonds

From the previous sections it follows that making a distinction between specific and non-specific bonds based on their strengths is not feasible for the discussed system. Therefore the initial fraction of non-specific bound beads should be minimized. By changing the preparation process of BSA or Biotin-BSA coated surfaces and the buffer solution in which the beads are contained, it is possible to reduce the number of beads binding non-specifically.

Experiments presented in this section have been performed on surfaces prepared using the process variant that led to the lowest number of non specific bonds. BSA and Biotin-BSA coated surfaces were prepared in the same way as described in section 4.1.2 except for the last step. In this process variant the substrates are first rinsed in ultra pure water before being blown dry. Incubating beads for 35s on a BSA surface prepared this way leads to an N_0 of 5 whereas on a Biotin-BSA surface it leads to an N_0 of 50. The non-specific over specific ratio is thus approximately 10%.

Although the fraction of non-specific bonds is small, it is important to understand the influence of the non-specific bonds on the results of constant force measurements on the Biotin-Streptavidin bonds. It is thus important to investigate the effect of different constant forces on the non-specific bonds. In figure 4.4 the percentage of non-specific bound beads is given as a function of time for different applied forces, N_0 is scaled to 100%. Except for the 18 pN force most nonspecific beads are removed from the surface within the 160 s of force application. That in the case of the 18 pN force the decay is slower than for the higher forces matches with the idea that the application of a force stimulates bond dissociation also when the bond is non-specific and can not be modeled by a single sharp energy barrier. For the other forces a relationship between the force and the timescale at which beads are removed from the surface does not follow from figure 4.4. Considering the low number of beads that is studied and the stochastic nature of bond

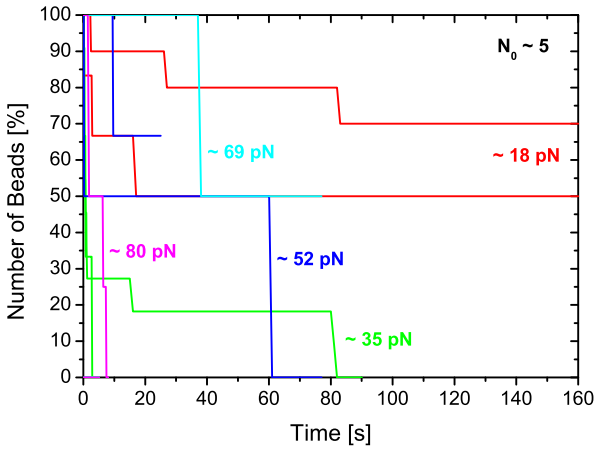

Figure 4.4: The effect of a constant force on Streptavidin coated beads bound to a BSA surface

breaking, such a relationship is however not likely to be derivable from the presented experimental results.

4.2 Constant Force experiments

The experiments presented in this section have been performed on Biotin-BSA coated surfaces prepared as described in section 4.1.3. This preparation process leads to an average fraction of non-specific bonds of 10% at a bead incubation time of 35 s and to a N_0 of about 50. After incubation of the beads, subsequently different constant forces have been applied to the beads and the number of beads bound to the surface is monitored as a function of time.

In figure 4.5(a) the percentage of bound beads is given as a function of time for different applied forces, N_0 is scaled to 100%. For every force the experiment has been performed two times. In every measurement a new surface and bead solution are used. In figure 4.5(b) the same data is presented as in figure 4.5(a) only this time, where possible, the results for two measurements at the same force are added to improve statistics. This time the total N_0 which is the addition of the N_0 values of the two separate measurements is scaled to 100%. This addition is allowed because the two measurements are performed under the same conditions. For comparison the theoretically expected first order exponential decay curves are also plotted in figure 4.5(b). These curves are obtained by using equations 2.22 and 2.28 with $t_{off} = 10^4$ s and $x_\beta = 0.41$ Å. These values are based on values

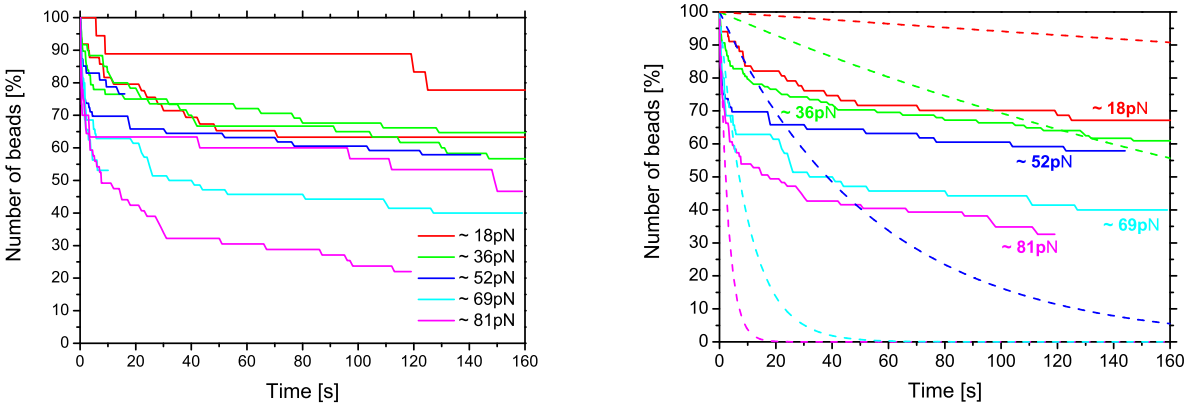

(a) (b)

Figure 4.5: The effect of different constant forces on Streptavidin coated beads Bound on a 0.04% Biotin-BSA surface. (a) Separate measurements. (b) Summated results (solid curves) and theoretically expected results (dashed curves).

measured by various techniques stated in reference [30] . There are three things to be addressed in this figure. The functional shape of the curves, the differences in results obtained for the same force and the force dependance of the dissociation rate.

If single molecular bonds are measured that dissociate irreversibly in a single step process, theory predicts a first order exponential decay (equation 2.28) in the number of beads that is bound as a function of time. Clearly this is not what is observed in figure 4.5. Not even when the statistical errors in the measurements are taken into account. The relative statistical error for these measurements, calculated as described in 4.1.2, is 10 - 15% at most in figure 4.5(a) and less than 10% for the added curves in figure 4.5(b). The measured initial decay is in general fast but at a certain point the decay slows down. Even at the highest force and after 160 s not all beads are removed from the surface. If two measurements are done at the same force but on different substrates (that are prepared in the same way), this leads to decay curves of a somewhat different shape. Both at 18 and at 81 pN the differences between the two curves are larger than statistically expected.

An explanation for the deviant functional shape is that not single molecular bonds are measured but a collection of beads that are bound with different numbers of bonds. The beads with only one bond cause the fast

decaying part in the measured curves and the beads bound by more than one bond cause the slower decaying parts. Beads that are bound by many Biotin-Streptavidin bonds, are not likely to come off the surface at all. This kind of decay is described by equation 2.34. If the fractions η_i vary for different surfaces or different areas of the same surface, this multiple bond model could also explain the differences between two measurements at the same force. An inhomogeneous distribution of Biotin-BSA over the surface could be the cause of variations in η_i. If two Biotin-BSA molecules are close to each other, it is possible that bonds are formed between Biotins from both BSA molecules and more than one Streptavidin on the bead.

That indeed multiple bond adhesions can cause large variations in the functional shape of the decay curves can be seen in figure 4.6. Here the theoretically expected decay curves are calculated for different ratios of the fractions of beads bound with 1, 2, and 3 bonds. The beads are assumed to be in a parallel configuration and break randomly (see section 2.3.4). Again $t_{off} = 10^4$ s and $x_\beta = 0.41$ Å are used as parameters.

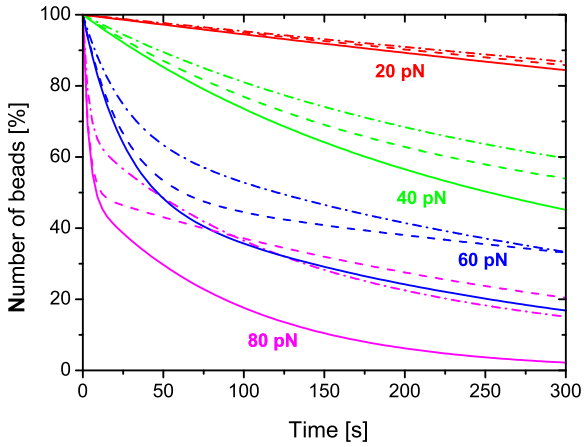

Figure 4.6: Dissociation of a collection of beads with different numbers of bonds. The fractions $\{\eta_1, \eta_2, \eta_3\}$ are varied. Solid curves $\{0.5, 0.5, 0\}$, dashed curves $\{0.5, 0, 0.5\}$, dash-dotted curves $\{0.33, 0.33, 0.33\}$. The colors correspond to the applied forces.

One thing that this model can not account for is the fact that for forces down from 52 pN the initial decay is faster than expected for a single Biotin-Streptavidin bond. This effect can partially be attributed to non-specific binding which is expected to comprise 10% of the total binding. In the 52 pN curve in figure 4.5(b) however the fast decaying fraction of beads is 30%. This could mean that there is a second effect that gives rise to bonds

weaker than the Biotin-Streptavidin bond. One idea is that due to surface roughnesses certain binding sites become less accessible or that the orientational freedom of some Biotin molecules is limited in such a way that partial bonds are formed. Partial bonds can be expected when multiple energy barriers and minima exist along the reaction coordinate of a specific bond. The presence of three energy barriers along the reaction coordinate of the Biotin-Streptavidin bond has been calculated in molecular dynamics simulations [42][43]. Experimental results have been obtained that support this picture [31][3]. A partial bond in this picture would correspond to a situation where the bound molecules are not in the primary energy minimum but in a minimum more outward along the reaction coordinate. The occurrence of this type of bonds has been discussed for the Biotin-Streptavidin system by Pincet and Husson [44].

The general trend in the decay curves as a function of time is as expected. The higher the force the faster the decay in the number of bonds as a function of time. Further interpretation in terms of fitting dissociation rate constants from the obtained curves is however difficult. In the first place because the number of collected data points is in most cases too small to fit higher order exponential behavior accurately. For quantification of dissociation rate constants many more dissociation events should be monitored. In the second place because it is hard to make out which type of bond corresponds with the fitted exponents.

To simplify the data analysis and interpretation, the probability of binding a bead by more than one bond should be reduced. Intrinsic problems with the Biotin-BSA - Streptavidin system are that one Streptavidin has four Biotin binding sites and that one BSA has multiple Biotins connected to it. There is thus a naturally high probability of binding by multiple bonds. Partially blocking Streptavidin binding sites with free biotin reduces the density of binding sites on the bead. This way the probability that a bead binds with multiple biotin molecules is reduced. Another solution is activating carboxylic acid beads with Biotin in a low density and adsorb Streptavidin on the polystyrene surface. Adsorption of the receptor molecules might however change their conformation and therefore their affinity for the ligand.

4.3 Multiple bonds

For the case of a 80 pN force some fits of second order exponential decay have been obtained which are accurate within a margin of 10%. Using the fitted dissociation rate constants for one and two bonds the multiple bond unbinding mechanism is further investigated.

In figure 4.7 the dissociation curves of two independent measurements are shown together with the fitted second order exponential decay curves

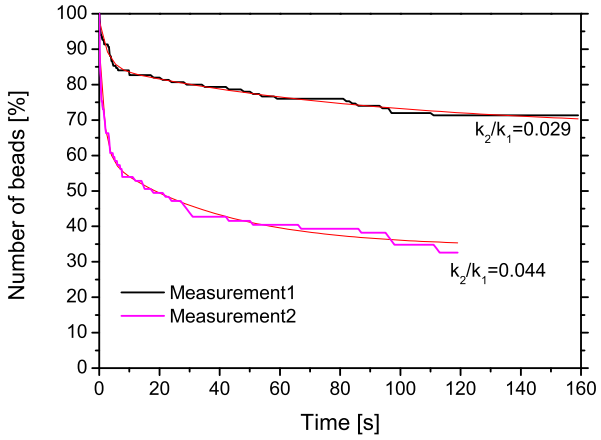

Figure 4.7: The effect of a force of $\sim$ 80 pN on Streptavidin coated beads bound on a Biotin-BSA surface.

(thin red lines). The black curve is obtained in an experiment in which the surfaces are prepared as described in section 4.1.2 and before the force of 80 pN is applied first a force of 10 pN is applied for 160 s to increase the fraction of beads that are specifically bound. Still in this case it can not be guaranteed that the fraction of non-specific bound beads is below 10%. The magenta curve is the same as the 81 pN magenta curve from figure 4.5(b).

In table 4.1 the fitted dissociation rate constants for one bond $k_d^1[s^{-1}]$ and two bonds $k_d^2[s^{-1}]$ are given and their ratio. The fitted dissociation rate constant for the case that first a 10 pN force was applied to the beads is approximately twice as low as for the case in which the force of 80 pN was applied immediately. This could be because in the first case the weakest bonds, which could be specific or non-specific, have already been removed. The order of magnitude of k_d^1 of 0.1 s^{-1} corresponds to values reported in literature [30]. In both cases the resulting ratio of k_d^2 over k_d^1 is in the order of magnitude of 0.01.

Table 4.1: Dissociation constants for beads bound with 1 bond, k_d^1, 2 bonds, k_d^2, and their ratio. Data derived from the curves presented in figure 4.7.

Measurement	$k_d^1[s^{-1}]$	$k_d^2[s^{-1}]$	$\frac{k_d^2}{k_d^1}[-]$
1	$3.73 \cdot 10^{-1}$	$1.07 \cdot 10^{-2}$	0.029
2	$5.92 \cdot 10^{-1}$	$2.60 \cdot 10^{-2}$	0.044

Using equations 2.29 to 2.33 and equation 2.21 the theoretically expected ratios of k_d^2 over k_d^1 are calculated for the different multiple bond configurations discussed in section 2.3.4. Here again the literature based values of t_{off} = 10^4 s and $x_\beta = 0.41$ $\mathring{A}$ are used. In table 4.2 the results are given. The ratio of k_d^2 over k_d^1 is highly dependant on the configuration of the bonds. As only the parallel configuration yields a result in the order of magnitude of the measured ratios it can be deduced that this is the configuration of the multiple Biotin-Streptavidin bonds. The Biotin-Streptavidin bonds between the bead and the surface are thus rendered parallel and break randomly.

Table 4.2: Ratios between dissociation constants for beads bound with one bond and beads bound with two bonds for the different cases of multiple bonds for different ways of multiple bond dissociation.

	parallel cooperative	series cooperative	parallel	zipper	series
theoretical $\frac{k_d^2}{k_d^1}$	$0.5{\cdot}10^{-15}$	$1.4{\cdot}10^{-12}$	0.035	0.5	2

Chapter 5

The Biotin - Anti-Biotin system

This chapter contains the results of measurements related to the Biotin - Anti-Biotin system. When compared to the Biotin-Streptavidin system the probability for binding by multiple bonds is less for this system, as Anti-Biotin has only two Biotin binding sites, and the Anti-Biotin molecules are expected to be less densely packed on the beads than the Streptavidin molecules. Two types of experiments have been performed with this system: Constant force experiments, described in section 5.1 and DFS experiments presented in section 5.2. In section 5.3 the results obtained from these experiments are compared.

5.1 Constant force experiments

Surfaces coated with BSA and Biotin-BSA are produced in the same way as for the constant force measurements on the Biotin-Streptavidin system. Dynal Dynabeads®M-270 Carboxylic Acid beads coated with Anti-Biotin are used in all experiments. The beads are contained in a buffer solution of 10 mg/ml BSA in PBS with 0.02% Tween20. After coating with Anti-Biotin many clusters were present in the bead solution, all beads in clusters are excluded from the experimental results.

For bead incubation times between 35 and 60 s, N_0, for this type of beads, is approximately 3 on a BSA surface. On a Biotin-BSA surface it is mostly higher than 30, however in some cases it was only 5. This is because of the presence of clusters. The number of non-specific bonds in this system is low, the strength on the other hand is very high. Most non-specific bound beads can not even be removed from the surface at forces up to 90pN. This is in contrast with the Streptavidin coated beads for which all non-specific bonds would break at such a high force when the same surface preparation process is used (see figure 4.4).

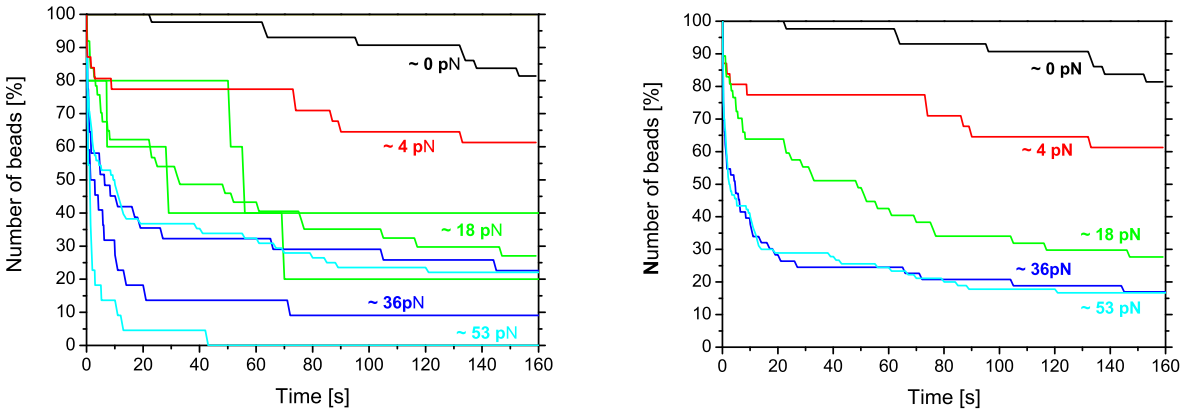

(a) (b)

Figure 5.1: The effect of different constant forces on Anti-Biotin coated beads bound on a 0.04% Biotin-BSA surface. (a) Separate measurements. (b) Summated results.

In figure 5.1(a) the percentage of bound beads is given as a function of time for different applied forces, N_0 is scaled to 100%. For some forces the experiment has been performed twice. In figure 5.1(b) the same data is presented as in figure 5.1(a) only this time, where possible, the results for two measurements at the same force are added up to improve statistics like has been done in figure 4.5(b). The relative statistical error for these measurements, calculated as described in 4.1.2, is 10 - 45% in figure 5.1(a) and less than 15% for the added curves in figure 5.1(b).

The measured curve for dissociation at zero force is expected to give an underestimation of the dissociation, because there is a time delay between the moment the sample holder is turned over after incubation of the beads and the moment the first image is collected. The first part of the exponential decay curve is thus not monitored. Furthermore as the beads are not pulled away from the surface very fast it is possible that, after dissociation, re-association takes place leading to a slower decay in the number of beads on the surface.

5.1.1 multiple bonds

As was the case for the Biotin-Streptavidin system here again the measured, dissociation curves do not follow first order exponential decay and again the results of measurements at the same force but at different samples do not overlap. As with the Biotin-Streptavidin system the multi-exponential

behavior can be explained by the formation of multiple bonds per bead. The problem of binding by multiple bonds is thus not solved by the change in receptor molecule only. Based on the fact that still Biotin-BSA is used and that Anti-Biotin has two binding sites for Biotin, it is possible that one Anti-Biotin binds to two Biotin molecules. It is also possible that two Anti-Biotin molecules bind with Biotins attached to one or more BSA molecules. The last mentioned effect will however be much smaller than when Streptavidin coated beads are used, as the concentration of Anti-Biotin on the bead surface is expected to be much lower. When the concentration of receptor on the bead is lower, the probability that two separate receptors bind with Biotin on the surface is lower. This could explain that the number of beads that do not come off at all (expectedly beads bound by many bonds) is lower than for the Biotin-Streptavidin system. Variations in the surface concentrations of Biotin-BSA and Anti-Biotin might cause sample to sample variations.

The general trend in the decay curves as a function of time is as expected, except for the fact that there is no significant difference between the curves measured at 36pN and 53pN. According to equations 2.22 and 2.28 the rate of dissociation should increase exponentially with the applied force. That this is not measured might be due to the fact that the observed amount of bond breaking events and thus the accuracy of the measurements is too low. As was the case for the Biotin-Streptavidin system, quantitative data analysis and interpretation is difficult because of the inaccuracy of the measurements and presence of beads bound by multiple bonds.

To really solve the problem of multiple bonds, a receptor should be chosen that has only one binding site for its ligand. Furthermore the ligand and receptor should both be bound to the surface homogeneously at a low concentration. When Biotin-BSA is used the average concentration of Biotin can be low but still the local concentration is high. This is an unwanted effect, single ligands or receptors should be diluted.

5.1.2 Strength of the BSA-polystyrene bond

When compared to the Biotin-Streptavidin system a faster dissociation of the Biotin - Anti-Biotin bond is expected, as the affinity of Streptavidin for Biotin is larger than that of Anti-Biotin. An observation that confirms this is that, in contrast to Streptavidin coated beads, Anti-Biotin coated beads even detach from the surface when no magnetic force is applied to the beads. However the curves that are measured at higher forces, for example at a force of 18pN are similar for the Biotin-Streptavidin system and the Anti-Biotin system. The only thing that is significantly different is the number of beads that does not dissociate at all. For the rest the time dependance in the dissociation curve is the same. Therefore the possibility should be considered, that not the dissociation of the Biotin-Streptavidin

and Biotin - Anti-Biotin bond, but the dissociation of BSA from the surface was measured.

There are indications that (Biotin-)BSA is attached stronger to the surface than the measured ligand-receptor pairs are attached to each other. In the first place the dissociation rate constants for the Biotin-Streptavidin system derived in section 4.3 are consistent with literature values. In the second place there are experiments presented in literature [30], where the same surface immobilization procedure for Biotin was used. In these experiments differences could be observed between closely related ligand receptor pairs, indicating that dissociation of BSA did not trouble the measurement results. Still the assumption that BSA does not come off the surface in this specific project should be verified. This can be done by varying the method of surface immobilization of Biotin. If the dissociation of actual ligand-receptor pairs is measured, the found dissociation rates should not depend on the method of surface immobilization.

To be sure that bonds between both the ligand and the surface, and the receptor and the bead are stronger than the studied bond, the coupling to both the bead and the surface should be covalent. It is possible to chemically activate polystyrene in order to have carboxylic acid or amino head groups on the surface [45]. To these groups receptors and ligands can be covalently coupled for instance by the EDC reaction described in section 3.3.2.

5.2 DFS experiments

In the Dynamic Force Spectroscopy experiments presented in this section, a force is applied to the beads that starts at 0 pN and is increased in steps to approximately 80pN at a steady loading rate. The number of beads leaving the surface between force f and $\triangle$f is recorded. The distribution of bond breaking events over the rupture forces has the shape of $p(\tilde{f})$, the rupture probability, given by equation 2.26.

5.2.1 specificity, reproducibility and accuracy

DFS experiments have been performed on two different sets of surfaces prepared in the same way as those used in the previous section. Also two different batches of beads have been used, both prepared as described in section 3.3.2 and appendix [A]. Although the preparation process was not changed, there were differences between the surfaces prepared in different sets and beads prepared in the different batches.

The most clear difference is that in the first batch of beads no clusters were present while in the second batch there were many clusters that could not be separated by sonication.

Differences between the surfaces prepared in different sets become clear when beads are incubated on them. When beads from the first batch were

incubated on surfaces prepared in set one for 90 s, this leads to an N_0 of 5 in case only BSA is present and an N_0 between 10 and 60 on a surface with 0.04% Biotin-BSA. Considering these numbers one would estimate the specific fraction on a Biotin-BSA surface to be 50 - 90 %. When the beads from the second batch are incubated on surfaces prepared in set two for 90 s this leads to an N_0 of 60 for both surfaces with only BSA and surfaces with 0.04% Biotin-BSA. Here specific binding can thus not be guaranteed. When beads from the first batch are now incubated at a BSA surface from the second set for 90 s this leads to an N_0 of 40. The amount of non-specific binding is thus almost ten times more on surfaces from the second set than on surfaces from the first set. From this it can be concluded that in the preparation of surfaces in the second set something went wrong in the process.

To check if there are differences in non-specific bond strength between beads from the different batches, a force is applied at a loading rate of 1 pN/s to beads from the second batch and beads from the first batch on BSA surfaces from the second set (on which many beads bind). Once the force had reached 80 pN, 90% of the beads from the first batch were removed from the surface while only 30% of the beads from the second batch were removed from the surface, (data not shown). Thus except from the clustering there are more differences in the properties of beads prepared in different batches.

Although the number of bonds on the Biotin-BSA surfaces prepared in the second set is not higher than on the BSA surfaces, it could still be that (some of) these bonds are specific. To test this, a force is applied at a loading rate of 1 pN/s to beads bound on both surfaces. The number of beads dissociating at a certain force is recorded. The force at which the most beads leave the surface is the most probable rupture force, f^*. It is expected that this most probable rupture force for the non-specifically bound beads is different than for specific bound beads. If now for beads bound on the Biotin-BSA surface an additional peak in the rupture probability shows up that is not present for beads bound on the BSA surface, this would support that at least some of the beads on the Biotin-BSA surface are specifically bound.

In figure 5.2 the results of these measurements are shown. At each surface the measurement has been repeated twice and the results are added to improve statistics. From the results presented in figure 5.2, no clear difference between the beads bound on BSA and the beads bound on Biotion-BSA can be observed. Therefore measurements done on surfaces prepared in the second set are not included in the next section where the results of DFS measurements are described.

The total number of bond breaking events n, monitored in these experiments and the ones presented in the next section is about 50, which might be low to visualize the total probability distribution for bond breaking. It is therefore hard to accurately define the location of maxima in the

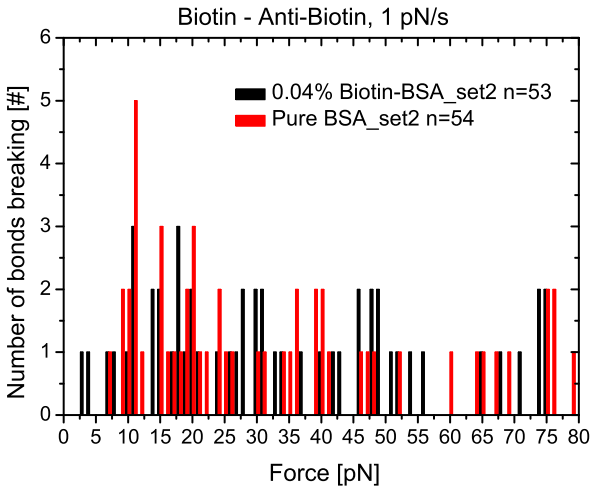

Figure 5.2: The number of bead dissociation events as a function of force at a constant loading rate of 1 pN/s on a surface with Biotin and a surface without Biotin.

probability distribution. The distribution might furthermore be blurred by non-specifically bound beads. Another factor limiting the accuracy of the presented measurements is the assumed relation between the voltage applied to the coil and the force on the beads. This relation is assumed to be linear, where in fact it is slightly nonlinear and depends on the temperature of the coil. Furthermore the voltage is increased in steps that are bigger for higher loading rates. The influence of all these effects is not investigated in detail and and/or compensated. The measurements presented here should thus be regarded as a proof of principle. Derived physical parameters should be valued as order of magnitude estimations.

5.2.2 results

DFS experiments have been performed on Anti-Biotin coated beads bound to a Biotin-BSA covered surface at five different loading rates between 0.1 pN/s and 10pN/s. The histograms with the recorded rupture events are given in figure 5.3. The width of the bars at high loading rates is larger than at low loading rates as the force resolution is less. However the number of events monitored per loading rate is low, the maxima in the probability distributions are estimated. For the loading rate of 0.1 pN/s one maximum is observed at approximately 2 pN, so 2 ± 1 pN is taken as an estimation. A second peak is observed at 14 ± 2 pN. For the loading rate of 0.2 pN/s

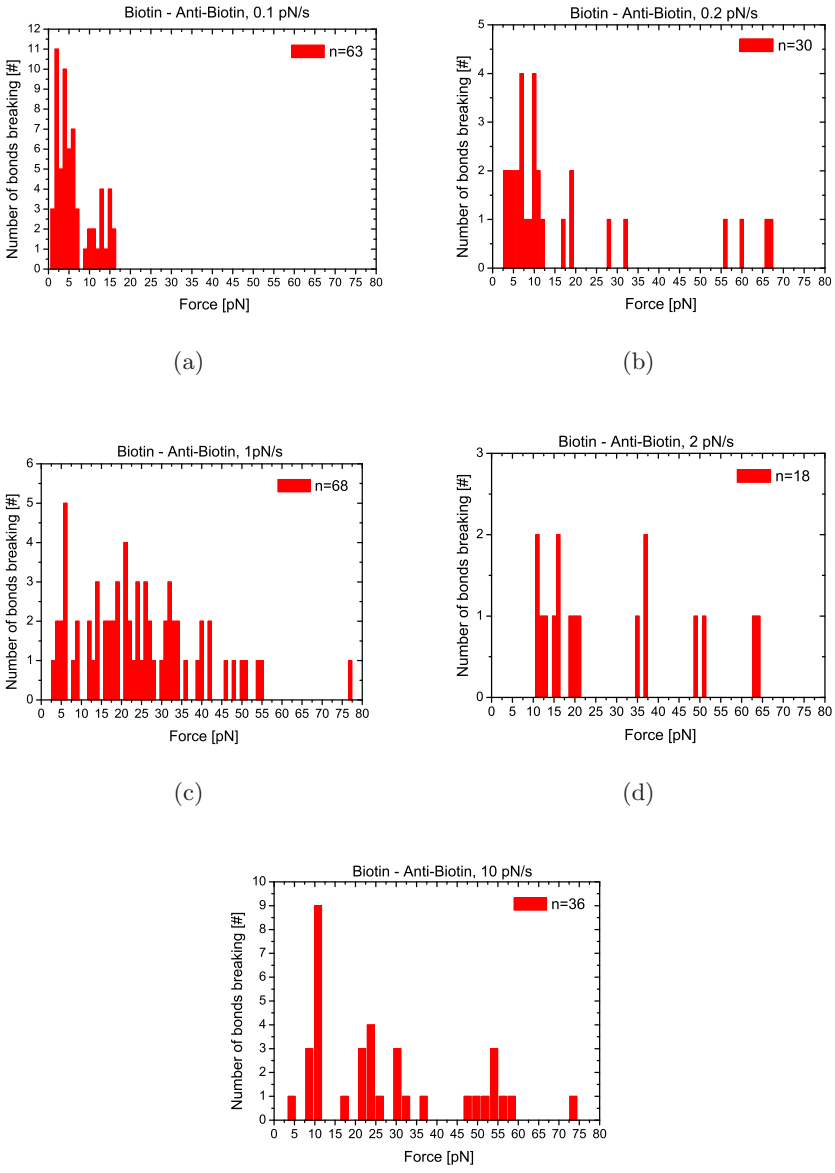

Figure 5.3: Histograms of bead dissociation events for different loading rates.

a maximum is a little harder to define but should be somewhere between 5 and 11 pN so 8 ± 3 pN is taken as an estimation. In the distribution at 1 pN/s roughly two maxima can be seen. One at 6 ± 2 pN and one at 21 ± 2 pN. For the loading rate of 2 pN/s the number of bond breaking events is too low to give a verdict about the positions of maxima. In the distribution at 10 pN/s three maxima can be observed: 0ne at 11 ± 2 pN, one at 23 ± 5 pN and one at 53 ± 5 pN.

It is possible that some of the peaks mentioned are artifacts. However for peaks corresponding to a specific type of bond, the forces at which the peaks occur would satisfy equation 2.27. If a set of peaks corresponds to a molecular bond, a linear relation between the peak force an the the natural logarithm of the loading rate should be observable. To test if this is the case, all the estimated peak forces are plotted in a graph versus the natural logarithm of the loading rate. The result is given in figure 5.4. Three sets of data points can be defined for which a linear fit can be made and which thus possibly are connected with a molecular bond. From the linear fits of these sets of data points the parameters x_β and k_{off} can be derived by rewriting equation 2.27 as

$$f^* = \frac{k_B T}{x_\beta} \ln r_f + \frac{k_B T}{x_\beta} \ln \frac{x_\beta}{k_B T k_{off}} \tag{5.1}$$

and equating $\frac{k_B T}{x_\beta}$ to the slope of the fit and equating the loading rate at zero force to $\frac{x_\beta}{k_B T k_{off}}$. The resulting values for x_β and k_{off} are given in table 5.1.

The fact that three different sets of data are found that can be fitted linearly, could mean that three different types of bonds are measured. It is also possible that these sets do not correspond to a certain type of bond at all, as some of the measured peaks might be artifacts and the sets consist of only three data points.

The second set of data could correspond to a bond that has a faster apparent dissociation at zero force and also a stronger force dependance than bonds possibly corresponding to the other data sets as its barrier is located more outward along the reaction coordinate. The found barrier positions can be compared with the barrier positions found for another other ligand-IgG bond. For the Digoxigenin-antibody bond, barriers are reported at 0.35 and 1.15 nm [46]. The barrier position found for the first set of data points is close to that of the first barrier in the Digoxigenin-antibody bond. However, in measurements on the Digoxigenin-antibody bond this barrier is only observed at loading rates higher than 10^3 pN/s. Therefore the barriers are not directly comparable. The positions of the second and third set are in the same order of magnitude as the second barrier in the Digoxigenin-antibody bond but somewhat more outward.

Although the second set of data corresponds to the fastest dissociating bond it is not clear if it is related to a single Biotin - Anti-Biotin bond. It

might also correspond to a partial Biotin - Anti-Biotin bond as its x_β is far from the primary energy minimum. The third set of data corresponds to a barrier that is located between the barriers from set one and two but is higher than both of them, as the dissociation rate at zero force corresponding to this barrier is much lower. Again the nature of the bond corresponding to this set is not clear.

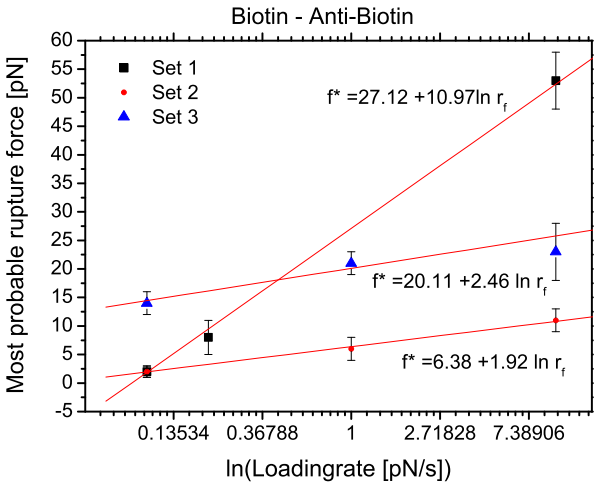

Figure 5.4: Derived values for f^* plotted versus the natural logarithm of the loading rate and possible linear fits of these data (Set 1 = 2, 8, 53 pN) (Set 2 = 2, 6, 11 pN) (Set 3 = 14, 21, 23 pN).

Table 5.1: Fitted values for x_β and k_{off}.

	Set 1	Set 2	Set 3	Thomas e.a.
x_β [nm]	0.37	2.1	1.7	unknown
k_{off} $[s^{-1}]$	$7.7 \cdot 10^{-3}$	$1.9 \cdot 10^{-2}$	$1.1 \cdot 10^{-4}$	$5.8 \cdot 10^{-6}$

A dissociation rate constant for goat Anti-Biotin has been determined by Thomas e.a. [47] with a technique in which labeled Biotin is injected in a column with Anti-Biotin immobilized on a solid support. The concentration of bound biotin is measured as a function of the time. Compared to the value determined by Thomas e.a. the dissociation rate constants determined in this research are very high. The difference could be caused by the fact that in this project both the Biotin and the Anti-Biotin are bound to a solid support instead of only the Anti-Biotin. Increased [48] as well as

decreased [49] dissociation rates as a consequence of surface immobilization are reported in literature. It is possible that when increased dissociation rates are measured, orientational constraints of the constituents of the bonds make it harder for them to reach their energetically most favorable relative position and orientation which could lead to weaker bonds. Furthermore attachment to a surface may induce changes in the protein structure of the Anti-Biotin leading to a different affinity for Biotin. Another explanation for an increased dissociation rate is that by the application of a force a certain reaction path is chosen that is not the most probable path if no force is applied.

5.3 Comparison of DFS and constant force experiments

The parameters calculated from the DFS experiments on the Biotin - Anti-Biotin system can be substituted in equation 2.28 to see what the theoretical outcomes of constant force measurements would be for these parameters. This has been done and the resulting dissociation curves are compared with the actual measurements at constant forces. To be able to make a better comparison, the beads that do not come off the surface at the highest force are not taken into account. The fraction of beads that is still bound to the surface after applying a force of 53 pN for 160s is approximately 15%. In each measurement, this fraction of N_0 is subtracted from the number of beads present at each time. The remaining 85% is scaled to 100%. In figure 5.5 the calculated curves as well as the measured curves are plotted. For calculation of the dashed curves the fitted parameters from the first set are used, for the dotted curves parameters from the second set are used, for the thin full curves parameters from the third set are used.

The decay that follows from the parameters of set one and two is much faster than the measured decay. When the parameters of the third set are used the decay at low forces is much slower than measured. The force dependence of the dissociation rate however is very strong so the decay for forces above 18pN is much faster than measured.

With some goodwill the curves calculated from set one can be said to match the initial rate of decay. The mismatch for the lower forces can be ascribed to the earlier mentioned time delay between the end of incubation and the start of the measurement. This could mean that the calculated parameters correspond to a single specific bond. Parameters that could correspond to the slower decaying fraction of beads are not measured in the DFS experiment.

The discrepancy is worse for the parameters from set two and three. To whichever type of bond these parameters correspond, this type of bond should, if it turns up in DFS experiments, also turn up in constant force

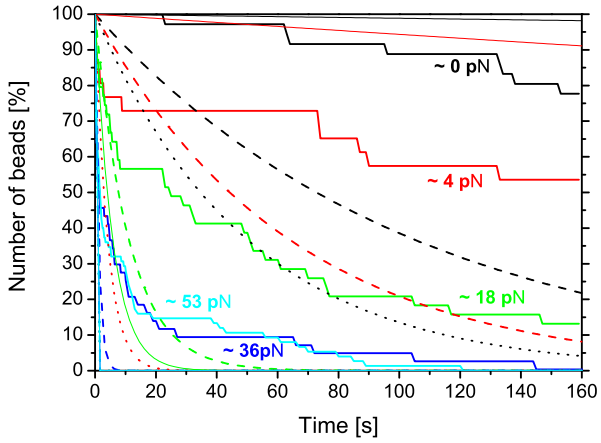

Figure 5.5: Comparison of constant force measurements and calculations based on DFS results, (dashed curves = set 1, dotted curves = set 2, thin full curves = set 3). The colors correspond to the applied forces.

experiments. The fact that this does not happen can be ascribed to either irreproducibility in the measurements or over-interpretation of the DFS data. Measurements with more beads and at more and higher loading rates are needed to verify which peaks are significant.

Chapter 6

Conclusions

The presented research aims to contribute to the development of a magnetic biosensor in which the strength of bonds between an antigen and an antibody can be measured. For this purpose a setup has been designed in which the force induced dissociation of antigens and antibodies can be measured. Section 6.1 describes the general conclusions of this project. Section 6.2 discusses the possibility of implementing a similar setup in a biosensor.

6.1 General conclusions

With the developed setup, magnetic forces up to 90 pN can be applied to superparamagnetic beads with a diameter of 2.8 μm. These forces are sufficient to break molecular bonds on a timescale of minutes. Furthermore dynamic force spectroscopy experiments can be performed with the present setup. Loading rates up to 10pN/s have been applied, however by using a different power supply higher loading rates can be obtained. An advantage of this setup over other techniques is that both constant force measurements and DFS measurements can be done in the same setup for an ensemble of bonds simultaneously.

With this setup the bonds between Biotin and Streptavidin, and Biotin and Anti-Biotin have been studied. In most of the experiments the number of bond breaking events was still too low to obtain quantitative information about the bonds. It is possible to bind up to 200 beads in the region of interest of the setup without beads getting too close to each other. When all these bead dissociate the maximum standard deviation in constant force measurements is 7%. In the Biotin-Streptavidin case the average number of beads that bind in the region of interest is 50. In the Biotin - Anti-Biotin case this number is only 30. The maximum standard deviations in most of the measurements on these systems were between 10 and 20%. An extra problem in the Biotin - Streptavidin case is that, with the present surface chemistry, only a small fraction of the initially bound beads disso-

ciates. The fraction of dissociating beads can be increased by decreasing the surface concentrations of Biotin and Streptavidin. An unwanted effect of this is that the total binding probability will decrease and so will the number of initially bound beads. This problem can only be solved by a longer incubation or an incubation that is stimulated by actuation of the beads. A longer incubation however could also lead to an increased number of non-specific bonds which is again an unwanted effect. For the Biotin - Anti-Biotin system not only the low number of bond breaking events, but also bead clustering and irreproducibilities in the bead coating procedure, troubled the measurements.

Although the biochemistry in the conducted experiments was not optimal, some hypotheses have been derived about the binding and dissociation of the studied bonds. Here it is assumed that the BSA via which the Biotin is coupled to the surface is not released from the surface during the measurements. There are indications that this assumption is valid, nevertheless it still should be verified.

⇒ The main conclusions for the Biotin-Streptavidin system are:

- The bond strength of Streptavidin coated beads non-specifically bound to a BSA coated polystyrene surface can be much weaker than a Biotin-Streptavidin bond but also stronger.
- Constant force measurements on the Biotin-Streptavidin system have shown that Dynal M-270 Streptavidin coated beads often bind to a surface with Biotin-BSA with more than one specific bond. The fractions of beads bound with a certain number of bonds vary per measurement due to surface inhomogeneities. A fast decaying fraction of beads is observed that is not expected from literature. Possibly this fraction of beads is only partially bound.
- The dissociation rate increases with the applied force.
- In an analysis of the shape of the dissociation curves at a force of 80 pN the configuration of the multiple specific bonds between a bead and a surface was obtained. The Biotin-Streptavidin bonds between the bead and the surface are rendered parallel and break randomly.

⇒ The main conclusions for the Biotin - Anti-Biotin system are:

- The bond strength of Anti-Biotin coated beads non-specifically bound to a BSA surface is higher than the Anti-Biotin bond. The number of non-specific bonds on a correctly prepared BSA surface is however low.
- Constant force measurements on the Biotin - Anti-Biotin system have shown that also Dynal M-270 Anti-Biotin coated beads often bind to

a surface with Biotin-BSA with more than one specific bond. However the average number of bonds per bead is lower than for the Biotin-Streptavidin system.

- As was the case for the Biotin-Streptavidin system, the dissociation rate increases with the applied force.

- From DFS measurements possible dissociation rates at 0 force and barrier positions are derived for the Biotin - Anti-Biotin system. The found dissociation rates at 0 force of, $7.7 \cdot 10^{-3}$, $1.9 \cdot 10^{-2}$ and $1.1 \cdot 10^{-4}$ s^{-1}, are all much faster than the dissociation rate of $5.8 \cdot 10^{-6}$ s^{-1} reported in literature. Possible barriers are found at 0.37, 2.1 and 1.7 nm from the primary energy minimum.

- The dissociation measured in constant force experiments does not correspond to what would be expected from the parameters derived from DFS experiments. Possibly the data obtained in DFS experiments is insufficient to be interpreted correctly.

Concluding, a setup has been developed in which the strength of antigen-antibody bonds can be tested using superparamagnetic beads. Measurements on the Biotin - Anti-Biotin bond an the Biotin-Streptavidin bond have shown that the dissociation rate constant of these bonds increased with the applied force and that the most probable rupture force shifts when different loading rate are used. Deriving more quantitative information from the conducted measurements was difficult because of the occurrence of multiple bonds per bead, the low number of beads dissociating and irreproducibilities. These causes are mostly of biochemical origin. For better results optimization of the biochemistry is essential. In specific, alternatives for the use of BSA in the surface immobilization procedure of Biotin should be tested. Furthermore, for a more quantitative analysis of the force dependence of the dissociation rate, more data should be collected. In constant force measurements the dissociation of a larger number of beads should be measured over a longer time. DSF experiments should be performed at more different and higher loading rates and a larger number of beads should be studied per loading rate.

6.2 Implementation in a biosensor

In the present setup both constant force and DFS can be done. Both can be implemented in a biosensor. This biosensor will however not be a hand held device that can be used anywhere. The magnetic system and power supply can not easily be miniaturized.

Implementation of constant force measurements is the most obvious option as the output of these measurements can be easily correlated to the

dissociation rate constant. In a biosensor application it is not necessary to obtain detailed information on parameters like x_β. Quantifying bond strength can in principle be done by measuring the number of beads at only one constant force. Once for a specific system the force dependance of the dissociation rate is know, this can be used to select a force at which the measurements should be done in order to have the best sensitivity in the range over which the dissociation rate constants are expected to vary. To be sensitive in a larger range of bond strengths measurements at different forces can be done. When the dissociation rate constant of an antigen-antibody pair is naturally high, measurements can be done at lower forces. The maximum dissociation rate constant that can be measured depends on how fast the number of beads on the surface can be detected. The accuracy of the biosensor is determined by the number of dissociating bead. The more dissociating beads can be measured simultaneously the more accurate the biosensor.

In a biosensor application the beads on the surface will not be detected with a microscope. Still optical detection is a possibility. For instance, a CCD can be mounted directly above the surface. Also magnetic detection is a possibility. The magnetic field of the developed set-up in the region of interest is perpendicular to the surface and a GMR sensor under the surface would only detect the parallel components of the magnetization of the beads.

In this project an antibody has been coupled to the surface of a super-paramagnetic bead. In a biosensor it it not feasible to isolate the antibody and do a coupling reaction. The bead and surfaces in the sensor should be pre-prepared so that the number of process steps in the sensor is minimized and the detection speed is optimized. The challenge here would be to bind sufficient beads to the surface to probe the probability distribution for dissociation accurately in one measurement. The use of smaller beads can be considered to obtain more beads per surface area. Smaller beads usually have a lower magnetic content so only smaller forces can be applied to them. The force that is needed to break bonds on a timescale of minutes varies per antigen-antibody pair. Therefore whether smaller beads can be used depends on which antigen-antibody pair should be characterized.

Based on the order of magnitude of antigen-antibody bond strength to be studied and the availability of other receptors or binding possibilities for the studied molecules, the specific method of measuring the bond strength should be chosen.

Bibliography

[1] M. Megens and M. Prins. Magnetic biochips: a new option for sensitive diagnostics. *Journal of magnetism and magnetic materials*, 293:702–708, 2005.

[2] K. van Ommering. Magnetic properties of sub-micrometer superparamagnetic beads used for biosensors. Master's thesis, Eindhoven University of Technology, 2005.

[3] R. Merkel, P. Nassoy, A. Leung, K. Ritchie, and E. Evans. Energy landscapes of receptor-ligand bonds explored with dynamic force spectroscopy. *Nature*, 397:50–53, January 1999.

[4] D. Leckband and J. Israelachvili. Intermolecular forces in biology. *Quart. Rev. of Biophys.*, 34:105–267, 2001.

[5] U. Piran and W. J. Riordan. Dissociation rate constant of the biotin-streptavidin complex. *J. Imm. Meth.*, 133:141–143, 1990.

[6] http://faculty.washington.edu/stenkamp/stefanieweb/abstract.html.

[7] P. C. Weber, D. H. Ohlendorf, J. J. Wendoloski, and F. R. Salemme. Structural Origins of High-Affinity Biotin Binding to Streptavidin. *Science*, 243:85–88, January 1989.

[8] T. F. Tadros, editor. *Colloid Stability.* Wiley-VCH, 2007.

[9] C. J. van Oss. *Interfacial Forces in Aqueous Media.* Dekker, 1994.

[10] P. J. Gellings and H. J. M. Bouwmeester, editors. *The CRC Handbook of Solid State Electrochemistry.* CRC press, 1997.

[11] B. Conway J. Bockris and E. Yeager, editors. *Comprehensive Treatise of Electrochemistry.* Plenum press, 1980.

[12] H. D. Abruna, editor. *Electrochemical Interfaces.* VCH Publishers, 1991.

[13] D. Grasso, K. Subramaniam, M. Butkus, K. Strevett, and J. Bergendahl. A review of non-DLVO interactions in environmental colloidal systems. *Rev. in Env. Sc. and BioTech.*, 1:17–38, 2002.

[14] K. L. Johnson, K. Kendall, and A. D. Roberts. Surface Energy and the Contact of Elastic Solids. *Proc. R. Soc.*, 324:301–313, September 1971.

[15] S. Freitag, L. Trong, L. Klumb, P. S. Stayton, and R. E. Stenkamp. Structural studies of the streptavidin binding loop. *Protein Science*, 6:1157–1166, 1997.

[16] P. Bondgrand. Ligand-receptor interactions. *Rep. Prog. Phys.*, 62:921–968, May 1999.

[17] P. R. Edwards and R. J. Leatherbarrow. Determination of Association Rate Constants by an Optical Biosensor Using Initial Rate Analysis. *Analytical Biochemistry*, 246:1–6, March 1997.

[18] G. Scatchard. The attractions of proteins for small molecules and ions. *Ann. N.Y. Acad. Sci.*, 51:660–672, 1949.

[19] D. Wild, editor. *The immunoassay Handbook*. Elsevier, 2005.

[20] E. Evans. Probing the Relation Between Force, Lifetime and Chemistry in Single Molecular Bonds. *Annu. Rev. Biophys. Biomol. Struct.*, 30:105–128, June 2001.

[21] S. Arrhenius. The attractions of proteins for small molecules and ions. *Z. Phys. Chem.*, 4:226, 1889.

[22] H. A. Kramers. Brownian motion in a field of force and the diffusion model of chemical reactions. *Physica*, 7:284–304, April 1940.

[23] G. I. Bell. Models for the Specific Adhesion of Cells to Cells. *Science*, 200:618–627, May 1978.

[24] C. Gergely, J. Hemmerle, P. Schaaf, Horber. J. K. H., J. Voegel, and B. Senger. Multi-Bead-and-Spring Model to Interpret Protein Detachment Studied by AFM Force Spectroscopy. *Biophys. J.*, 83:706–722, August 2002.

[25] G. Hummer and A. Szabo. Kinetics from Nonequilibrium Single-Molecule Pulling Experiments. *Biophys. J.*, 85:5–15, 2003.

[26] M. Panhorst, P. Kamp, G. Reiss, and H. Bruckl. Sensitive bondforce measurements of ligand-receptor pairs with magnetic beads. *Biosensors and Bioelectronics*, 20:1685–1689, 2005.

[27] A. Ptak, M. Kappl, and H. J. Butt. Modified atomic force microscope for high-rate dynamic force spectroscopy. *APL*, 88:263109, 2006.

[28] E. Evans, K. Ritchie, and R. Merkel. Sensitive Force Technique to Probe Molecular Adhesion and Structural Linkages at Biological Interfaces. *Biophys. J.*, 68:2580–2587, June 1995.

[29] B. Brower-Toland, C. L. Smith, R. C. Yeh, J. T. Lis, C. L. Peterson, and M. D. Wang. Mechanical Disruption of Individual Nucleosomes Reveals a Reversible Multistage Release of DNA. *PNAS of USA*, 99:1960–1965, January 2002.

[30] C. Danilowicz, D. Greenfield, and M. Prentiss. Dissociation of Ligand-Receptor Complexes Using Magnetic Tweezers. *Anal. Chem.*, 77:3023–3028, May 2005.

[31] A. Pierres, D. Touchard, A. Benoliel, and P. Bongrand. Dissecting Streptavidin-Biotin Interaction with a Laminar Flow Chamber. *Biophys. J.*, 82:3214–3223, June 2002.

[32] G. Zocchi. Force Measurements on Single Molecular Contacts through Evanescent Wave Microscopy. *Biophys. J.*, 81:2946–2953, November 2001.

[33] C. Zhu, M. Long, S. E. Celcea, and P. Bongrand. Measuring ReceptorLigand Interaction at the Single-Bond Level: Experimental and Interpretative Issues. *Annal. Biomed. Eng.*, 30:305–314, 2002.

[34] M. O. Budnick and R. S. Fitzgerald. New life for a diagnostic reagent mainstay. *DVI Technology*, pages 45–52, June 2003.

[35] G. Sagvolden. Protein Adhesion Force Dynamics and Single Adhesion Events. *Langmuir*, 14:5984–5987, August 1998.

[36] G. Sagvolden, I. Giaever, and J. Feder. Adsorption/desorption of human serum albumin at the surface of poly(1actic acid) nanoparticles prepared by a solvent evaporation process. *Biophys. J.*, 77:526–532, 1999.

[37] T. Verrecchia, P. Huve, D. Basile, M. Veillard, G. Spenlehauer, and Couvreur P. Characteristic Protein Adhesion Forces on Glass and Polystyrene Substrates by Atomic Force Microscopy. *J. Biomed. Mat. Res.*, 27:1019–1028, 1993.

[38] G. Fonnum, C. Johansson, A. Molteberg, S. Mørup, and E. Aksnes. Characterisation of dynabeads by magnetization measurements and mössbauer spectroscopy. *Journal of magnetism and magnetic materials*, 293:41–47, 2005.

[39] P.M.M. Rombouts. Superparamagnetic bead rotation for biosensor applications. Master's thesis, Eindhoven University of Technology, 2007.

[40] The different types of streptavidin-coupled dynabeads. http://www.invitrogen.com/content.cfm?pageid=11113.

[41] B. D. Matthews, D. R. Overby, F. J. Alenghat, J. Karavitis, Y. Numaguchi, P. G. Allen, and D. E. Ingber. Mechanical properties of individual focal adhesions probed with a magnetic microneedle. *Biochem. Biophys. Res. Com.*, 313:758–764, 2004.

[42] S. Izrailev, S. Stepaniants, M. Balsera, Y. Oono, and K. Schulten. Molecular dynamics study of unbinding of the avidin-biotin complex. *Biophys. J.*, 72:1568–1581, 1997.

[43] H. Grubmuller, B. Heymann, and P. Tavan. Ligand Binding: Molecular Mechanics Calculation of the Streptavidin-Biotin Rupture Force. *Science*, 271:997–999, February 1996.

[44] F. Pincet and J. Husson. The Solution to the Streptavidin-Biotin Paradox: The Influence of History on the Strength of Single Molecular Bonds. *Biophys J.*, 89:4374–4381, December 2005.

[45] G. U. Lee, S. Metzger, M. Natesan, C. Yanavich, and S. F. Dufrene. Implementation of Force Differentiation in the Immunoassay. *Anal. Biochem.*, 287:261–271, 2000.

[46] G. Neuert, C. Albrecht, E. Pamir, and H. E. Gaub. Dynamic force spectroscopy of the digoxigeninantibody complex. *FEBS Letters*, 580:505–509, 2006.

[47] D. H. Thomas, D. J. Rakestraw, J. S. Schoeniger, V. Lopez-Avila, and Van Emon J. Selective trace enrichment by immunoaffinity capillary electrochromatography on-line with capillary zone electrophoresis - laser-induced fluorescence. *Electrophoresis*, 20:57–66, 1999.

[48] V. H Perez-Luna, M. J. O'Brien, K. A. Opperman, P. D. Hampton, G. P. Lopez, L. A. Klumb, and P. S. Stayton. Molecular Recognition between Genetically Engineered Streptavidin and Surface-Bound Biotin. *J. Am. Chem. Soc.*, 121:6469–6478, 1999.

[49] H. Nygren and M. Stenberg. Immunochemistry at Interfaces. *Immunology*, 66:321–327, 1989.

Acknowledgements

I am grateful to the following people: Arthur de Jong for supervising my project. Loes van Zijp for her work in the biochemical lab. Martijn Kemerink for performing AFM measurements. Thea van der Wijk and Toon Evers of Philips research for advising me on the biochemistry part of my project. Kim van Buuren for giving me a hamster home. Asha Jacob for the continuation of my project. Xander Janssen for teaching me soldering and LabView programming. Francis Farni for showing me how to use Comsol. Menno Prins and Leo van IJzendoorn for their advise and pep-talks. All students of the MBx group for being good company. And my boyfriend Michael for always being there for me.

Appendix A

Protecol for binding Anti-Biotin to Carboxyl acid beads

Necessities

- 25 mM MES (2-(N-morpholino)ethanesulfonic acid) buffer (pH=5)
- 100 mM MES buffer (pH=5)
- EDC
- 50 mM ethanolamine in PBS (pH=8.0)
- Assay buffer (= 0.02% Tween and 10 mg/ml BSA in PBS)
- Anti-Biotin 1 mg/ml, 50 μl
- Bead solution (M270 Carboxylic acid beads, Dynal), 100 μl

Protocol

1. Wash the beads
    - Pipette 100 μl of bead solution in a LowBind-ep
    - Pull beads toward the side of the ep with a magnet
    - Replace the liquid with the same amount of 25mM MES buffer
    - Mix well and repeat this procedure 4 times
    - Suck out most of the liquid (to obtain a concentration of about 5:1)
2. Add anti-Biotin

- Add 50 μl of anti-Biotin solution
- Incubate dynamically for 30 minutes at room temperature

3. Couple the anti-Biotin to the beads

   - Prepare a 100 mg/ml EDC solution in 100 mM MES
   - Add 10 μl of the EDC solution to the beads
   - Mix well
   - Add 10 μl 25 mM MES buffer
   - Incubate dynamically for 2 hours at room temperature

4. Quench the reaction

   - Add ethanolamine solution to the bead solution ($\sim$900 μl)
   - Incubate dynamically for 1 hour at room temperature

5. Remove the excess of EDC/anti-Biotin

   - Suck out most of the liquid
   - Wash the beads once with ethanolamine solution
   - Wash the beads 4 times with assay buffer

Appendix B

Bead counting software

Program to count beads in subsequent frames of a movie (single .tif files) The first frame will be shown and the beads must be selected manually. The program registers if a beads is still at its postition in subsequent frames and gives the number of beads still left in each frame as an output.
Inge van Donkelaar, July 2007, MBx

```
Select file to analyze
    clear all
    close all
    [filename,path]=uigetfile('*.tif','open .tif-file');
    name=filename(1:max(size(filename))-10);
    I=(imread(strcat(path,name,num2str(0,'%06d'),'.tif')));

Show first frame and register bead locations by mouse clicks
    colormap(gray(256));
    image(I) [inputx,inputy]= getpts;

count beads/input points
    beads = size (inputx,1)
    beadsN = beads;
    delta(1)=0;
    for n=0:53 %for 0 to number of frames-1 compare frame with the next
frame
    I=double(imread(strcat(path,name,num2str(n,'%06d'),'.tif'))); %frame
    I2=double(imread(strcat(path,name,num2str(n+1,'%06d'),'.tif'))); %next
frame
    for j=1:size(inputx,1) %for all bead locations/centres
    x0(j) = round(inputx(j)); %integer bead x coordinate
    y0(j) = round(inputy(j)); %integer bead y coordinate
    int= 0; %intensity 0
```

```
    int2= 0; %intensity 0
    for x = [x0(j)-8:x0(j)+8]
    for y = [y0(j)-8,y0(j)-7,y0(j)-6,y0(j)-5,y0(j)-4,y0(j)-3,y0(j)+3,y0(j)+4,
    y0(j)+5,y0(j)+6,y0(j)+7,y0(j)+8]
    int = int+I(y,x); %add pixel values in frame
    int2 = int2+I2(y,x); %add pixel values in next frame
    end
    end
    d = double(abs(int-int2)); %compare added up pixel intensities
    if d > 5000 %if the difference between the intensities at a certain location
has changed more than a threshold value this means a bead has disappeared
    beadsN = beadsN-1; %in that case the number of beads in the 'next
frame' is lowered by 1
    end
    end
    beads=[beads,beadsN]; %the number of beads in subsequent frames (length(beads)
= number of frames)
    delta(n+2)=beads(n+1)-beads(n+2); %the number of beads dissociating
in subsequent time frames (length(delta) = number of frames)
    end

Output
    name %file name
    beads'
    plot (beads, 'DisplayName', 'beads', 'YDataSource', 'beads'); figure(gcf)
%the number of beads present on the surface plotted versus frame number
    delta'
    plot (delta, 'DisplayName', 'delta', 'YDataSource', 'delta'); figure(gcf)
%the number of dissociating beads plotted versus frame number
```